Fall 1-31-2002

Shear behavior of reinforced concrete deep beams strengthened with CFRP laminates

Jon Erik Moren
New Jersey Institute of Technology

ABSTRACT

SHEAR BEHAVIOR OF REINFORCED CONCRETE DEEP BEAMS STRENGTHENED WITH CFRP LAMINATES

By
Jon Erik Moren

Considerable research has been performed using CFRP plates bonded to normal reinforced concrete beams, the objective being to improve shear and flexural strength. However, very few tests have been performed on reinforced concrete deep beams with CFRP as shear reinforcement. The purpose of this experiment is to investigate the behavior of the deep beam in shear with various arrangements of Sika CarboDur laminates bonded to the sides. The beams were designed to be shear deficient with stirrups omitted, except at the supports and directly under the load. In total eight beams were tested, four with one-point loading and four with two-point loading. Each loading condition contained one control beam without CFRP, and three beams with the CFRP laminates attached at zero, forty-five, and ninety degrees with respect to the neutral axis. The ultimate loading capacity and behavior for each beam bonded with the CFRP laminate was observed and recorded.

The mode of failure was shear in all the beams tested, which typically resulted from the delaminating between the concrete and the epoxy. The present test results show that the orientation of the CFRP about the neutral axis had a direct effect on the shear strength of the beam and its ductility. The forty-five degree alignment of CFRP plates gave the greatest increase in shear capacity and ductility, whereas the ninety-degree alignment gave the least amount.

SHEAR BEHAVIOR OF REINFORCED CONCRETE DEEP BEAMS STRENGTHENED WITH CFRP LAMINATES

By
Jon Erik Moren

A Thesis
Submitted to the Faculty of
New Jersey Institute of Technology
In Partial Fulfillment of the Requirements for the Degree of
Master of Science in Civil Engineering

January 2002

APPROVAL PAGE

SHEAR BEHAVIOR OF REINFORCED CONCRETE DEEP BEAMS STRENGTHENED WITH CFRP LAMINATES

Jon Erik Moren

Dr. Cheng-Tzu Thomas Hsu, Thesis Advisor — Date
Professor of Civil Engineering, NJIT

Professor Edward G. Dauenheimer, Committee Member — Date
Professor of Civil Engineering, NJIT

Professor Walter Konon, Committee Member — Date
Professor of Civil Engineering, NJIT

BIOGRAPHICAL SKETCH

Author: Jon Erik Moren

Degree: Master of Science

Date: January 2002

Undergraduate and Graduate Education:

- Master of Science in Civil Engineering
  New Jersey Institute of Technology, Newark, NJ, 2002

- Bachelor of Science in Civil Engineering
  New Jersey Institute of Technology, Newark, NJ, 2001

Major: Civil Engineering

To my beloved family

ACKNOWLEDGMENT

I would like to thank my thesis advisor Dr. Cheng-Tzu Thomas Hsu for all of his insight, guidance, and financial support during my stay at NJIT. In addition, I'd like to thank my thesis committee members, Edward G Dauenheimer and Walter Konon for their contributions, and the entire Civil Engineering Department who have supported me immensely. I would also like to thank the Chairman of the Civil Engineering Department, Dr. John R. Schuring, and Graduate Advisor, Dr. Hsin-Neng Hsieh, for the opportunity to teach and attend school on a full-time basis. Special thanks to Allyn Luke for helping me to prepare and to execute the experiments for this thesis.

Thanks to the Sika Corporation and David White for the technical support and donation of the CFRP laminate and epoxy used in the experiments. Also I would like to thank Legge Industries and Marty Lucibello for donating all of the materials needed to fabricate and cast the beams.

I would also like to thank my wife, Debra, and the rest of my family for all of their love, support, and understanding during the last year. Without their support this master's degree would not be possible. I would also like to thank Ph.D. student, Zhichao Zhang, and fellow masters students, Sun Punurai and Voradej Vongvorakarn for all of their help with mixing and testing of the deep beams. I would also like to recognize my father, Jan Moren, for all his help in bending the steel for the re-bar cages. I know he had other things to do, but I really needed the help. Finally, thanks to all of those people that I forgot to mention.

TABLE OF CONTENTS

TABLE OF CONTENTS
(Continued)

TABLE OF CONTENTS
(Continued)

Chapter **Page**

LIST OF TABLES

LIST OF FIGURES

LIST OF FIGURES
(Continued)

LIST OF FIGURES
(Continued)

CHAPTER 1

INTRODUCTION

1.1 History/Literature Review

There is both a great interest and need in the United States and abroad to repair and strengthen structural elements such as columns, beams, and slabs within a particular building system. The primary reasons to upgrade and repair an existing structure include building code changes, accidents, design errors or building use changes. Currently, there are several options available to repair and strengthen existing structures in both flexure and shear.

For the past twenty-five years, the most popular method for strengthening and repairing structures is to epoxy-bond steel plates to the critical areas of the structure. The benefits are that the life cycle of the structure can be extended and that the cost of replacement of the structure can be avoided. The main drawbacks to this method are the amount of weight the steel adds to the structure, and the fact that steel rusts when exposed to harsh environments; therefore, is not suitable for all applications. In addition, the plates' weight requires the use of special tools and equipment to ensure proper installation.

The use of composite material such as GFRP and CFRP offer many advantages over steel. FRP has a high corrosive resistance and strength to weight ratio. Its light weight makes it easy to handle and install. The material has the additional benefit of being available in any length and the flexibility to be molded to match any surface irregularities. The major drawback to the use of FRP composites is their higher cost over steel, and the fact that they are

anisotropic, meaning they don't possess the same properties in each direction, as does steel. The first carbon FRP repair and strengthening system was introduced in Switzerland in 1984 by Meier, who remains an innovator in the field of FRP research. (1)

Over the last decade, FRP plates and fabrics have been used extensively in Europe and around the world to increase the moment capacity of flexural members. The first full-scale use of CFRP strengthening for flexure in the United States was in 1994 to rehabilitate a bridge in Wilmington, Delaware. (2) Since then the use of FRP composites has gained a wider acceptance in the United States, particularly in California were it has been used to update structures to meet new seismic code requirements. However, the use of FRP for shear reinforcement has not been as widely researched or applied. The reason is due to the nature of the shear failure itself. Unlike bending failure, which is ductile and gives a warning before failure, shear failure is brittle and occurs with little or no warning. For this reason, the ACI (American Concrete Institute) forbids the design of over-reinforced concrete structures in its design procedures. The rationale being that if the structure is under-reinforced, the occupants will be able to see that the structure is compromised by observing deflections or cracks, and therefore have an opportunity to evacuate the structure.

In the last two years, various papers have been published on the subject of shear reinforcement using CFRP composite materials. In 1999, Khalifa and Nanni, from the research lab at the University of Missouri at Rolla, published a paper titled "Improving shear capacity of existing RC T-section beams using

CFRP composites." Six full-sized simply supported beams were strengthened with various arrangements of CFRP sheets. The experimental results indicated that "externally bonded CFRP can increase the shear capacity of the beam significantly." (3) In that same year, Taljsten and Elfgren, from Lulea University of Technology in Sweden, published a paper on the research of the shear force capacity of beams before and after strengthening using CFRP fabrics and tapes. Their test results demonstrated that bonding CFRP fabrics to the face of the concrete beams increased the shear strength. (4) In 2000, Dr. Hsu and Ph.D. student Zhang at New Jersey Institute of Technology in New Jersey investigated the shear behavior and modes of failure for normally reinforced concrete beams strengthened with CFRP laminates. They concluded that CFRP could significantly increase the serviceability, ductility and ultimate strength of reinforced concrete beams. (5) However, after extensive research no information could be found on CFRP reinforcement on deep beams, thus the objective of my paper.

1.2 Objectives

The objectives of this experiment are to :

1. Investigate the ductility, shear behavior, and failure modes of reinforced concrete deep beams with shear deficiencies after strengthening with Sika CarboDur strengthening system.

2. To increase the database on shear strengthening using externally bonded CFRP laminates.
3. To determine the optimum configuration of CFRP laminates that will impart the greatest shear strength and increase in ductility.

CHAPTER 2

DESIGN, FABRICATION AND MATERIALS

2.1 Design of Reinforced Concrete Deep Beam

When designing a beam, there are three possible modes of failure that can occur: shear, bending and bond length. In order to investigate how the CFRP laminates benefit the shear strength of the beam, the beam must fail in shear. If the beam were to fail in bending or bond length, there would be no way of determining exactly how much strength the CFRP laminates contributed.

The deep beam was designed as an under-reinforced section in accordance with the American Concrete Institute (ACI) Building Code. (6) To guarantee that the mode of failure would be shear, horizontal and vertical shear reinforcement was omitted from the design, except in special circumstances discussed later. In practice, this is avoided because of the lack of warning and sudden nature of brittle failure. However, for this case, it was necessary in order to investigate how the CFRP plates improved the shear strength of the deep beam. The design for the beam is broken down into the following three areas : flexural, bond length and shear.

2.1.1 Flexural Design and Reinforcement

The beams designed for this experiment are considered to be normal beams in flexure, in accordance with ACI 10.7.1. ACI does not have a specific design procedure for beams with a height to clear span ratio greater than .8 and requires non-linear analysis to determine the flexural design. The height to clear span

ratio for the deep beam in the experiment is .3, which allowed the assumption of Whitney's Rectangular Stress Distribution to determine the flexural strength.

The flexural design calls for the use of four individual number four re-bar as reinforcement which represents a steel reinforcement ratio of .0250. This value is within the ACI maximum of seventy-five percent of the steel reinforcement at the balanced condition, which is equal to .0283. Figure 2.1 shows the location of the flexural and temperature control re-bar used in the experiment. The complete flexural design for the deep beam is located in Appendix A, ACI Reinforced Concrete Deep Beam.

2.1.2 Bond Length

A deep beam is a special case where the loading condition creates a multi-axial state of stress in the beam. The shear stresses and strains generated within a deep beam are non-linear and have components in both the X and Y direction. This state of multi-axial stress within the deep beam places a large amount of stress on the anchorage zone and the main tension reinforcement. (7) The development length for the tension bar terminating in a standard hook was determined by using ACI 7.1 and 7.2. A value of eleven inches was determined for the development length for both loading conditions. The calculations for the development length are furnished in Appendix A, ACI Reinforced Concrete Deep Beam Design.

2.1.3 Shear Design and Reinforcement

Shear is very important consideration when dealing with deep beam design. The ACI code 11.8 classifies a deep beam as having a clear span to depth ratio of less than five for a distributed loading condition. This translates into a shear span to depth ratio of 2.5 or less for concentrated loads. The beam designed for the experiment has a shear span to depth ratio of 1.88, which classifies it as a deep beam for shear by the ACI.

Special design procedures are required by the ACI when designing a deep beam for shear. They include the following recommendations : For a concentrated load, the critical distance for shear design is located at a distance .5 times the shear span length from the support. The use of a special multiplier is required when determining the shear carrying capacity of the concrete. This is due to the fact, that as the beam is loaded, a tied-arch effect occurs, which gives the concrete increased shear capacity even after shear cracks have formed. The ACI detailed method is used with the multiplier to calculate the shear capacity of the plain concrete in the experiment. The shear capacity of the beam for one- and two-point loading was calculated to be 15.8 kip and 24.0 kip, respectively. The calculations for the shear capacity of the concrete are furnished in Appendix A, ACI Reinforced Concrete Deep Beam Design.

The shear reinforcement provided in the beam consists of two individual number two stirrups at each support and one individual number two stirrup located directly under the load. This was done so that the beam would not experience local failure. In total, the one-point loading condition contained five

stirrups while the two-point loading condition used six stirrups. Figure 2.1 shows the arrangement of the shear and flexural reinforcement for each loading condition used in the experiment. Shear reinforcement was excluded from the beam in the areas where the CFRP was to be attached.

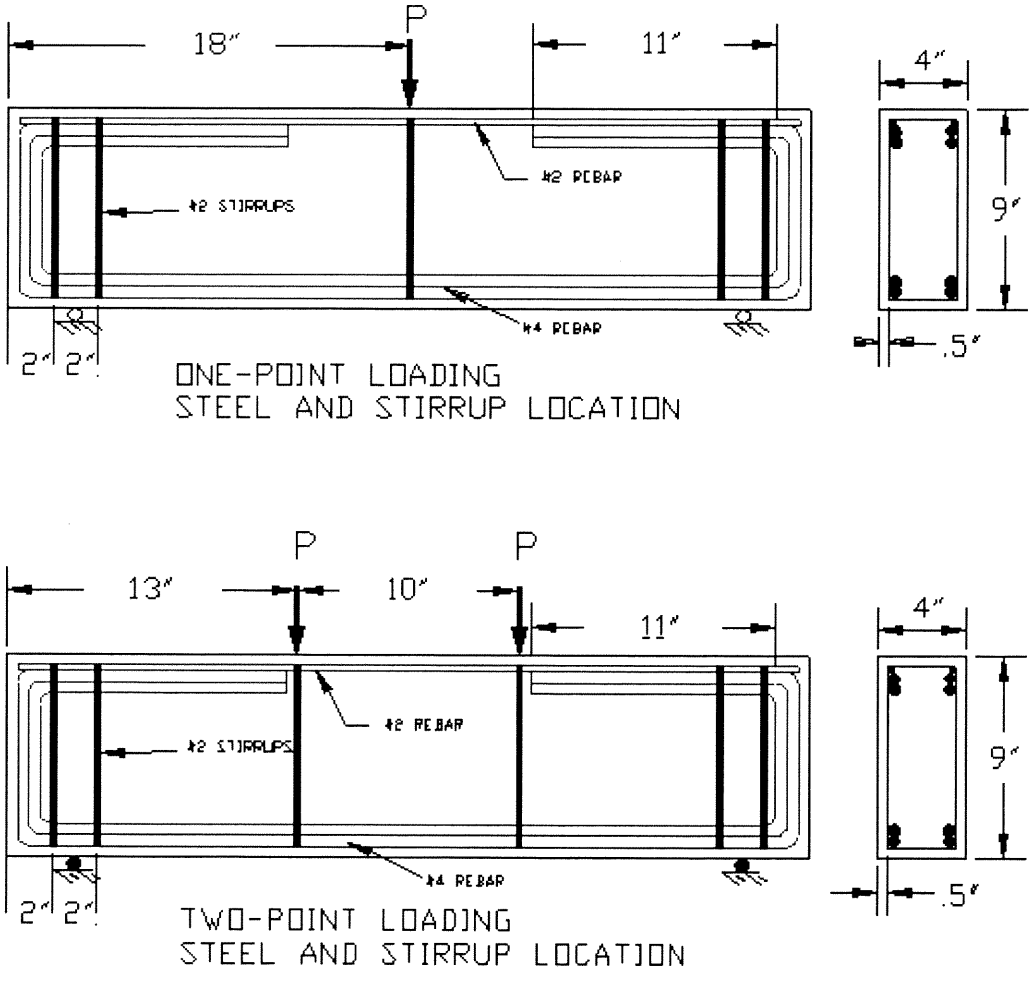

Figure 2.1 Shear and flexural reinforcement

2.2 Fabrication of Re-bar Cage and Forms

2.2.1 Fabrication and Assembly of the Re-bar Cage

The size of the beam designed gave some interesting fabrication problems. This was particularly evident in the area of bending the steel for the flexural reinforcement. The beam designed (three feet long, nine inches high and four inches wide) required that the steel be bent to very exacting tolerances. Many attempts were made to bend the steel by cold working, however, the end product was too distorted to use. An oxygen acetylene torch was then used to heat the steel so that it could be bent into the exact shape required. After some experimentation and fabricating specially designed forms, number two stirrups and number four flexural reinforcement re-bar were bent and cut to length. This was not in accordance with ACI recommendations, which require that all the steelwork be done cold. However, due to the small dimensions of the beam, it was unavoidable.

After the individual components of the beam had been fabricated, they were combined together to form the re-bar cage. (See Figure 2.2) Number two re-bar was used for temperature control at the top of the beam and also served as location points to attach the stirrups under the load. Standard tie wire was used to secure the stirrups and flexural reinforcement together.

In order to maintain the half-inch of clear cover around the steel reinforcement, a spot weld was used at the top of the stirrup to keep the re-bar cage from expanding. Under normal conditions, this is not recommended because it makes the stirrup continuous. However, it was necessary in order to

maintain proper spacing. To insure consistency from beam to beam, each stirrup within the beam was secured with a spot weld.

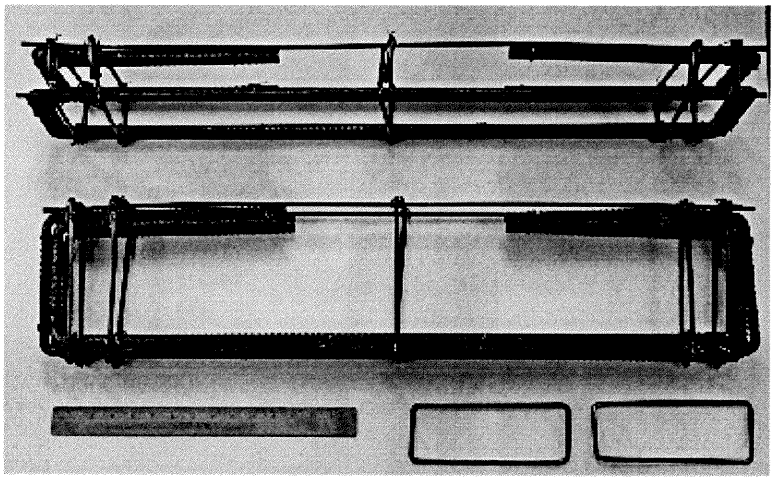

Figure 2.2 Re-bar cage assembly

2.2.2 Form Design and Construction

The forms were constructed from Grade A/A three-quarter inch pressure treated plywood to insure that the beams had a smooth surface on which to bond the CFRP laminates. The surfaces of the forms were painted with numerous coats of paint to protect the wood from the concrete. (See Figure 2.3) The forms were designed so that four beams could be cast simultaneously, which increased the consistency from beam to beam. This allowed all the beams from the same loading condition to be made with the same identical concrete mix, which eliminated a potential difference in strengths from beam to beam.

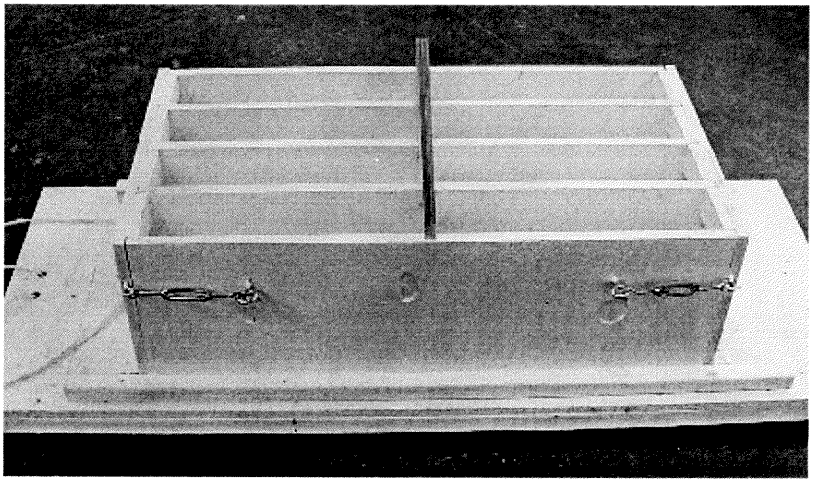

Figure 2.3 Forms for deep beams

2.3 Casting of Concrete Beams

2.3.1 Concrete Mix Design and Ultimate Strength

The concrete mix was designed in accordance with ACI 211 "Standard Practice for Selecting Proportions for Normal, Heavyweight, and Mass Concrete" which is based on the absolute volume method. A computer program called Mathcad was used to calculate the exact quantities and proportions needed for the design. Included in the mix proportions are enough concrete to fill five eight inch tall by four inch diameter cylinders, and four three foot by nine inch by four inch beams. Table 2.1 lists the batch requirements for one batch consisting of four beams and four test cylinders. The target strength for the mix design was five thousand pounds per square inch, with a water cement ratio of .41, and a predicted slump and air content of 3 inches and two percent, respectively. The entire mix design is located in the Appendix B, Concrete Mix Design and Test Cylinder Stress Strain Curves.

Table 2.1 Batch requirements

Ingredients	Quantities
Water	29.6 lbs.
Cement Type I	65.6 lbs.
Coarse Aggregate	159.7 lbs.
Fine Aggregate (3/8)	105.9 lbs.
Total Volume Required	2.5 cu.ft.

The cylinders were tested for compressive strength at the same time the beams were tested. The first batch contained five of test cylinder specimens and the second batch contained four. The results of the individual compressive tests are recorded in Table 2.2, and the average compressive strength for each batch is calculated. The average compressive strength was used to calculate the theoretical shear capacity of the concrete and the flexural strength of the beam. The stress-strain curves for the compressive cylinder tests are included in Appendix B, Concrete Mix Design and Test Cylinder Stress Strain Curves.

Table 2.2 Maximum compressive strength of concrete cylinders

Number of Cylinder	Ultimate strength f_c' (psi)	
	Concrete Batch 1	Concrete Batch 2
1	6526	6446
2	6367	6048
3	5570	5660
4	5809	6685
5	6446	X
Average	6143.6	6207.3

2.3.2 Casting Procedure

A six cubic yard mixer located in the Reinforced Concrete Lab at NJIT was used to mix the concrete for the beams in two batches. The first batch made was for the one-point loading condition, and the second for the two-point loading condition. The forms were well oiled to ensure that the sides of the beam would be smooth and free from imperfections. The re-bar cages were placed inside the forms and held in place by three-quarter inch square stock to ensure that the proper spacing was maintained. As the concrete was poured, a hand held vibrator was used to ensure the proper placement and consolidation of the concrete in and around the re-bar cage. The American Society for Testing Standard C 31 "Standard For Making and Curing Concrete Test Specimens in the Field" (6) was followed when making the five test cylinders for each batch.

2.3.3 Curing Procedure

After the beams and cylinders were cast, they were immediately transferred to a 100 percent humidity curing room for two days. After the second day, the forms were removed and the beams were returned to the curing room for an additional twenty-six days. On the twenty-eighth day, both the beams and the test cylinders were removed from the curing room. The beams were transferred to the testing facility to have the CFRP bonded to the surface. Figure 2.4 shows the beams and test cylinders curing in the curing room. These cylinders were tested at the same time the beams were tested to determine the compressive strength of the concrete at the time of the experiment.

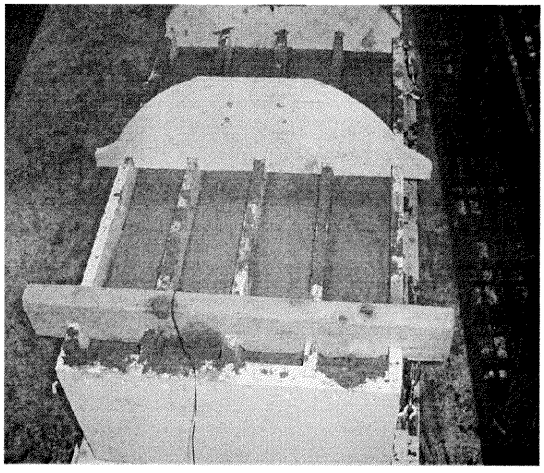
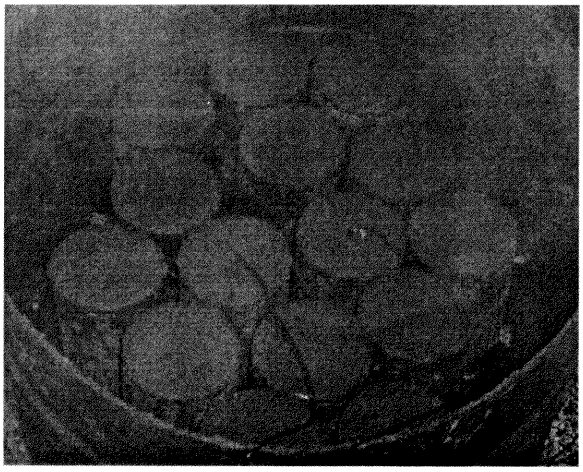

Figure 2.4 Beams and test cylinders curing

2.4 Sika CarboDur Strengthening System and Installation

The Sika CarboDur heavy duty strengthening system was used as the shear reinforcement for the deep beams in the experiment. It was selected based on its previous use in CFRP experiments at NJIT (5) and because of its familiarity and availability. The Sika CarboDur strengthening system is comprised of two components: Sikadur-30 adhesive bonding reinforcement and Sika CFRP laminates. (8)

2.4.1 Sika CFRP Laminate

The Sika CFRP laminates are comprised of a base of "Carbon fibre reinforced polymer with C fibres (Toray T 700) and an epoxy resin matrix." (1) The unidirectional carbon fiber strips come in two varieties : Type 50 with a 50-mm width and Type 80 with an 80-mm width. Each is available in one- and two-millimeter thickness and are available in any length desired. The Type 50 with one-millimeter thickness was selected as the laminate to be used as the shear

reinforcement for this experiment. The material arrived in one continuous length and was very easy to work with, requiring a pair of tin snips to cut the CFRP into the desired lengths. Table 2.3 lists properties of the Type 50 CFRP laminate.

Table 2.3 CFRP laminate properties

Properties	Sika CarboDur laminate
Description	Pultruded carbon Fiber Laminate
Tensile Strength	406,000psi (2,800 N/ mm^2)
Tensile Modulus	23.9msi (165,000 N/mm^2)
Elongation at Break	1.9%
Nominal Thickness	.047in. (1.2mm)
Tensile Strength per inch Width	19,082lbs./layer (84.5KN)

2.4.2 Sikadur-30 Adhesive

The other component of the Sika CarboDur strengthening system is Sikadur-30 adhesive for bonding reinforcement. "The purpose of the adhesive is to produce a continuous bond between fibre reinforced polymer (FRP) and concrete to ensure that full composite action is developed by the transfer of shear stress across the thickness of the adhesive layer."(1) Sikadur-30 is described as a "solvent free, thixotropic, epoxy-based 2-component adhesive."(9) A "pre-dosed" pack of Sikadur-30 was used for the experiment that consisted of two components, which were mixed together with a low speed electric mixer. Great care was taken to ensure that additional air was not introduced in the epoxy, which would reduce its effectiveness and strength. The final product was easy to manage for close to an hour and took on a light gray appearance similar to that of concrete. The properties of Sikadur-30 are given in Table 2.4.

Table 2.4 Sikadur-30 adhesive properties

Property	Sikadur-30
Compressive Strength	>95 N/mm^2
Adhesive Strength on Concrete	406,000psi (2,800 N/ mm^2)
E-modulus	23.9msi (165,000 N/mm^2)

2.4.3 CFRP Laminate Bonding Procedure

The hand lay-up technique for the installation of the CFRP laminate on the sides of the deep beam involved the following steps. The first and most critical step was to prepare the surfaces of the beams by grinding them smooth and removing any loose particles. A shop vacuum was used to remove any residual dust and particles from the surface of the beams. This was done to ensure that the epoxy had a good surface with which to bond. It is recommended by Sika that the surface of the beam be inspected and any large holes or imperfections filled with putty or a thick paste epoxy. However, the forms used to cast the beam worked very well in giving the beams a smooth finish and the number of blowout holes in the surface were small. It was decided, therefore, not to use any putty on the surfaces of the beams and to fill small holes with the Sikadur-30 adhesive at the time of installation.

Next, the CFRP laminate was cleaned with paint thinner (acetone based) to remove the carbonization layer. This was done to ensure the CFRP laminate maintained a good bond with the epoxy. Then the Sikadur-30 was prepared and applied in accordance with the manufacture specifications. In order to ensure

uniform coverage, the Sikadur-30 was applied to both the surfaces of the beam and to the back of the CFRP laminate with a putty knife. A roller was then used to press the CFRP laminate on to the beam allowing approximately one sixteenth to one eighth of an inch of adhesive to remain between the CFRP laminate and the surface of the beam. The excess epoxy was allowed to squeeze out from under the laminate and wiped off.

2.4.4 CFRP Laminate Spacing and Orientation

The ACI standard for shear reinforcement spacing was used as a guideline for determining how far apart to space the CFRP laminates on the beams. ACI 11.5.4.1 requires that stirrups not be placed greater than half the effective depth apart. This corresponds to a four-inch spacing requirement, which was used for all three CFRP laminate orientations. It should be noted Sika does not have a recommended spacing procedure for this application.

The following figures depict how the CFRP was arranged on the beams. A centerline to centerline spacing of four inches is used for both the forty-five and ninety-degree aligned CFRP laminates. More CFRP shear reinforcement was required for the one-point loading than the two-point loading due to the larger area of shear in the one-point loading case. The forty-five degree one-point loading case has six CFRP strips per side while the two-point loading case only requires only four CFRP strips per side. The ninety-degree case requires eight horizontally applied CFRP strips while the two point loading case requires only six per side. By inspection, it is obvious to see why there is less required CFRP

laminates for the two-point load due to the fact that there is no shear between the two loads.

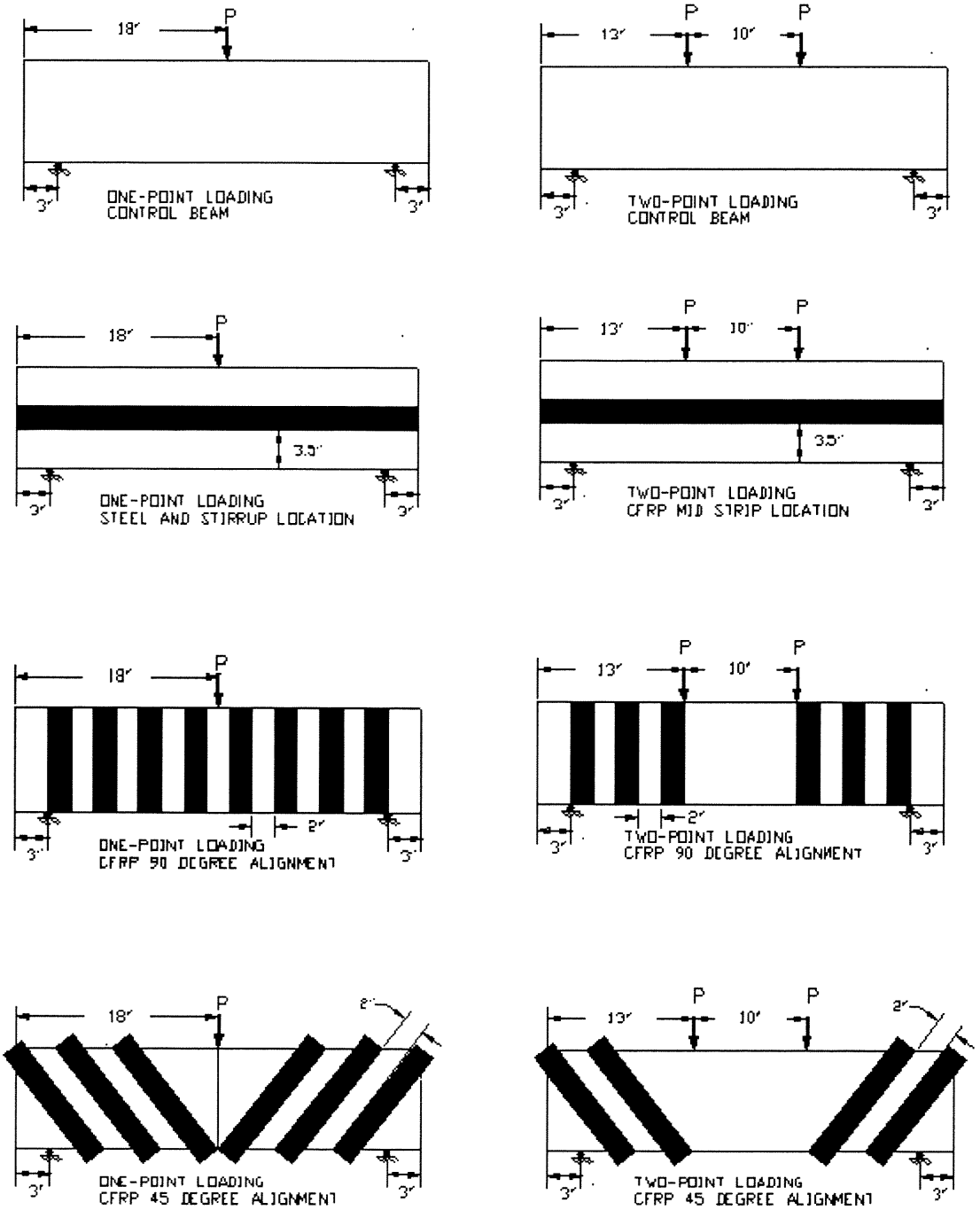

Figure 2.5 CFRP laminate alignment for deep beams

CHAPTER 3

CFRP REINFORCED DEEP BEAM TESTING

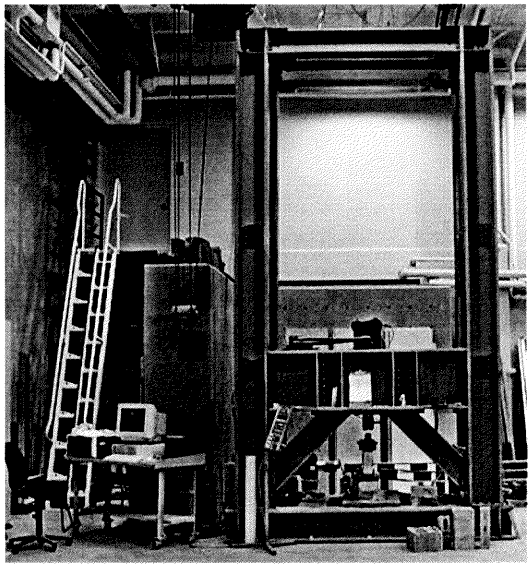

Figure 3.1 Reinforced concrete beam testing frame

3.1 Testing Equipment and Procedures

3.1.1 Testing Equipment

Located in the basement of the Architectural Building at NJIT is the reinforced concrete beam testing facility where the experiments were carried out. At the heart of the facility is a custom installed two-story frame, pictured above. (Figure 3.1) This frame has a high degree of stiffness and can be modified to accommodate different configurations of beams as well as other structural elements. All of the beams were tested using the MTS (Material Testing System), which is a closed loop servo hydraulic testing system controlled by the MTS test star digital system located within the frame. The maximum capacity of the load cell used in this experiment was fifty kips. The experiment was executed in load control with the automatic data acquisition system monitoring and recording both

the load and the deflection mid span. All of the beams were statically tested to fail in one loading cycle.

3.1.2 One- and Two-Point Loading Conditions

Each of the three-foot long beams to be tested was simply supported by two, two-inch diameter steel rollers located three inches from each end of the beam. A steel plate was inserted between the concrete and the steel roller to ensure that local failure did not occur at the support. It was necessary to place two four-inch thick concrete blocks under each support to elevate the beams so that the stroke of the testing machine could reach the specimen. For the one-point loading condition, a one-inch diameter steel ball bearing suspended between two steel plates was used to transfer the load evenly from the load cell to the surface of the test specimen. This same procedure was used with the two-point loading condition with one additional step. A special device was used to separate the load into two equal components exactly ten inches apart. The device is placed so that each load component is located five inches from the centerline of the beam. Figure 3.2 shows the typical set-up used for the one- and two-point loading conditions. The device located mid span under the beam is the external LVDT, which was used to measure the deflection of the beam as it was loaded.

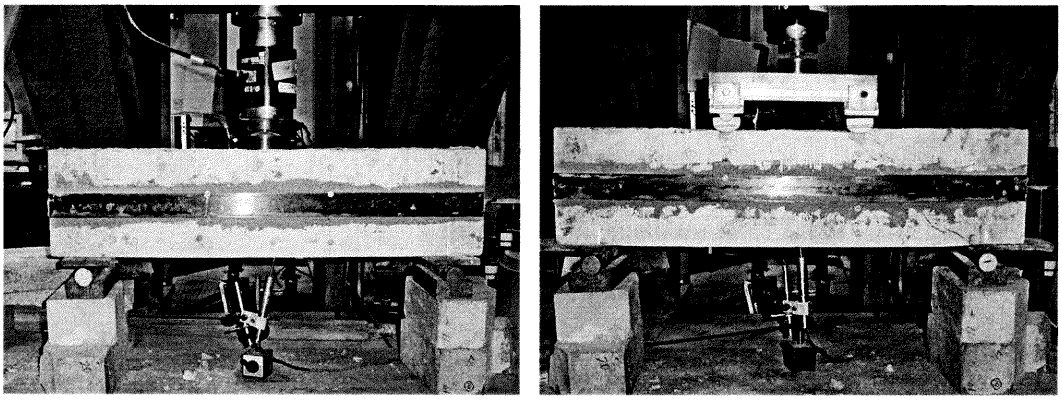

Figure 3.2 Typical example of one- and two-point loading

3.1.3 Moment-Curvature Curve

The ductility of the deep beams reinforced with the CFRP laminate was measured during the experiment by using a mechanical strain gauge. Four pairs of mechanical strain gauges, also known as demec gauges, were installed on the face of each of the beams tested. A typical arrangement of the demec gauges is shown in Figure 3.3. One set of gauges is located five inches to the right of the centerline of the beam, while the other set is located five inches to the left of the centerline. Each row pictured is approximately two inches apart and distributed evenly across the web of each beam.

Initial readings were taken with a mechanical strain gauge after a slight load was applied to the beam. Subsequent readings were taken in three kip intervals until the beam failed. The strain length change was determined and plotted versus its location on the face of the beam. The angle formed between the strain length change and its location on the face of the beam is the angle of curvature for the beam and was measured using excel. The angle of curvature was then used to

determine the radius of curvature for each of the beams tested. The radius of curvature is inversely related to the horizontal curvature of the beam and is a good indicator of ductility in beams. The shorter the radius of curvature the more curvature the beam experiences and this translates into increased ductility. By plotting the bending moment versus the longitudinal curvature of the beam, the ductility of the beam can be observed. By plotting all four of the moment-curvature curves on the same graph, the ductility between beams with different alignments of CFRP laminate can be compared.

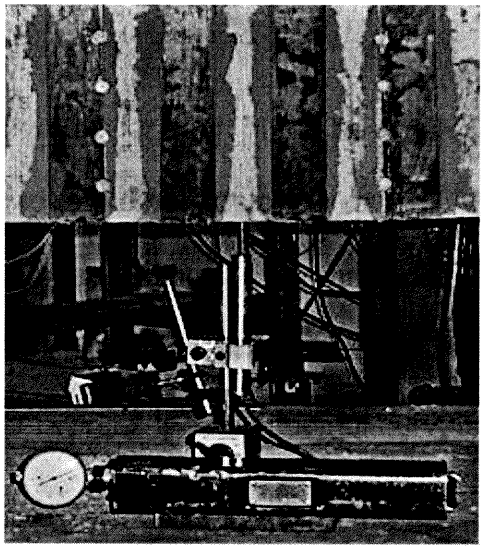

Figure 3.3 Mechanical strain gauge and demec gauge location

3.2 Behavior of Beams without Shear Reinforcement

3.2.1 General

The factors that influence shear behavior and strength in simply supported reinforced concrete beams are numerous and complex and not completely understood. These factors include the size and shape of the beam's cross

section, the quantity and arrangement of the flexural, compressive and transverse reinforcement, the shear span to depth ratio and the properties of the concrete and steel themselves. However, when factors other than the shear span to depth ratio are held constant for a rectangular cross section, the variation in the shear capacity can be illustrated by the Figure 3.4. (7)

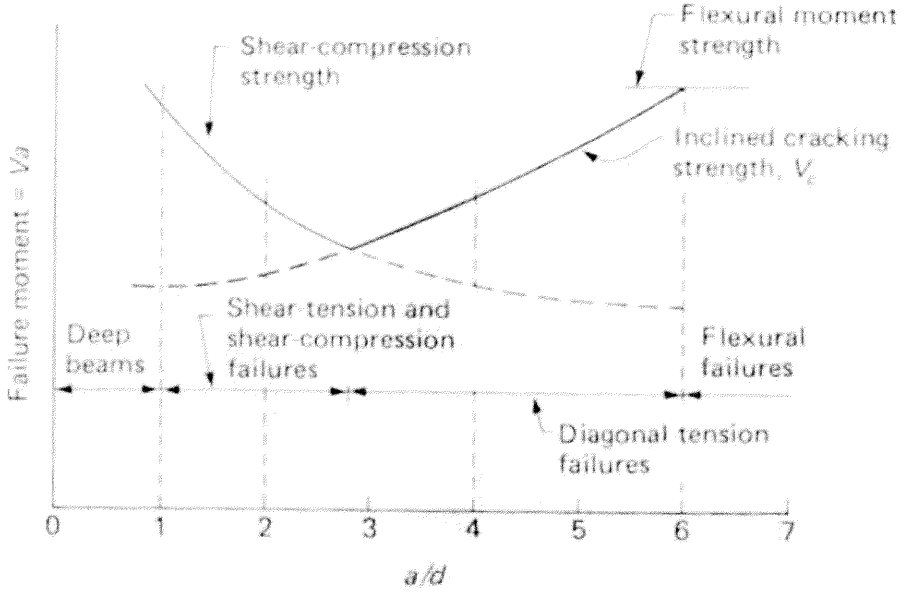

Figure 3.4 Variation in shear with a/d for rectangular beam (7)

This figure can be reduced into four main categories:

1. Deep beams, which possess a shear span to effective depth ratio of less than one.

2. Short beams, which possess a shear span to effective depth ratio greater than one but less than two point five.

3. Intermediate beams, which possess a shear span to effective depth ratio greater than two point five and less than or equal to six.

4. Long beams which, possess a shear span to effective depth ratio greater than six. (7)

For this experiment, the beam designed would be considered a short beam by traditional definition however, ACI classifies any beam with an shear span to effective depth ratio of less than two point five be designed as a deep beam. For the purpose of this experiment, only the deep beam and short beam shear behavior will be discussed.

3.2.2 Deep Beam Failures

For beams that have a shear span to depth ratio of less than one shear stress has the most effect. Once the inclined crack has formed, the beam behaves as a compressive tied arch, which has large reserve capacity; this allows the concrete of the beam to carry a larger shear capacity than a normal concrete beam. There are several modes of failure once the tied arch system has taken effect. They include anchorage, bearing, flexure, and arch-rib failure. Figure 3.5 part (a) shows the formation of the compression arch for a simply supported deep beam under two-point loading. Figure 3.5 part (b) labels and demonstrates the location of the failure zones that result after the compressive arch has formed.

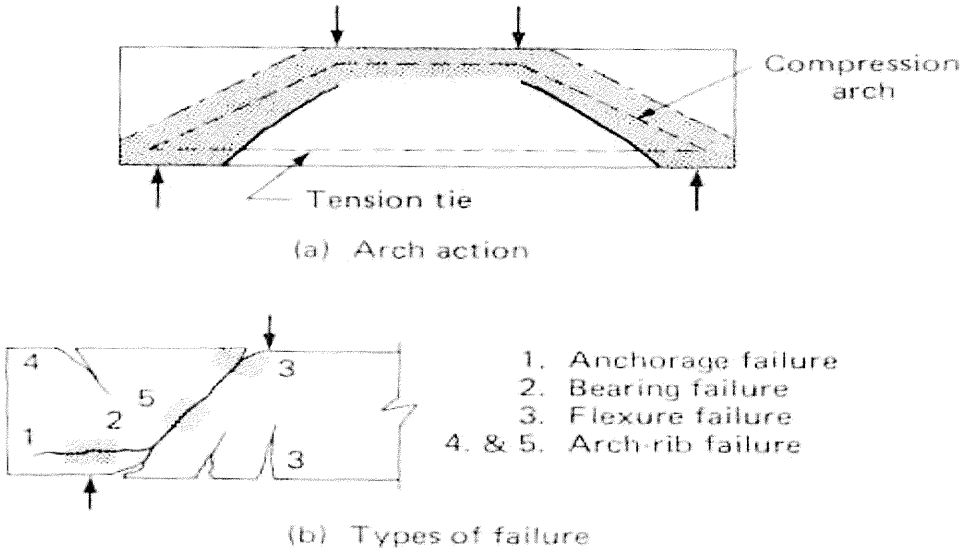

Figure 3.5 Modes of failure in deep beam (7)

3.2.3 Short Beam Failures

For beams that have a shear span to depth ratio between one and two point five, the shear strength exceeds the inclined cracking strength, just like a deep beam. When the beam is loaded, flexural-shear cracks develop which extend from the tension zone and continue to develop into the compression zone as the load is increased. Secondary cracks form along the tension reinforcement and progress toward the support. The failure may be either anchorage failure, at the tension reinforcement also known as “shear tension” failure, or the concrete in the compression zone directly under the load crushes known as “shear compression” failure. (7)(10) See Figure 3. 6.

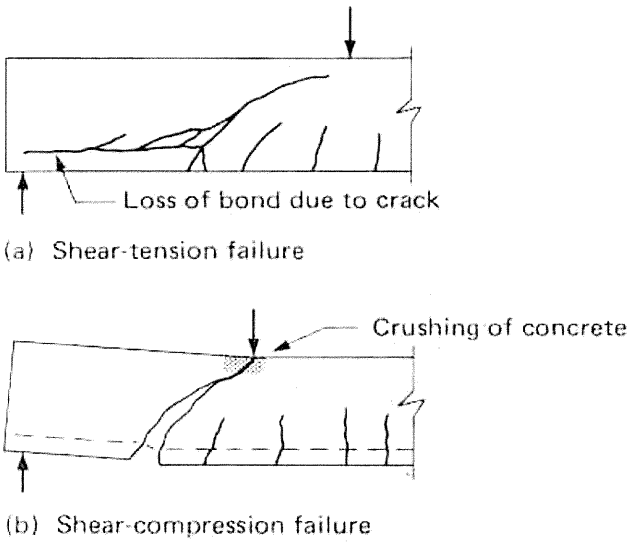

Figure 3.6 Modes of failure in short beam (7)

3.3 Behavior of Beams with CFRP Shear Reinforcement

There are four main failure mechanisms, which can limit the shear strength that the externally bonded CFRP laminate can contribute to the overall shear strength of the beam.

3.3.1 Concrete Bond Failure

The most common type of failure experienced occurs between the surface of the concrete and the epoxy. “In this failure mechanism, the Sika CarboDur plate debonds from the beam by shearing the surface of the concrete.” (1) With this particular failure mode the total shear strength of the CFRP laminate and epoxy is not completely utilized. The shear strength of the system is limited to the “ultimate bond strength of the concrete surface that anchors the FRP”. (1) A loud bang is accompanied by this failure mode which results from the CFRP laminate

delaminating from the beam. This failure is dramatic, with a large amount of energy released. Various models have been developed to explain the relationship among the bonding strength of the composites to the concrete surface. (11) (12) At this time, ACI does not have an approved method available to calculate the bond strength between the concrete and the epoxy.

3.3.2 Tensile Strength of CFRP Laminate

As previously mentioned, CFRP laminates are anisotropic and possess great bearing capacity in the direction that the fibers are laid. However, in the other direction it doesn't possess the same properties. The CFRP laminate loaded in its weak direction is easy to separate. In the application under consideration the failure of the CFRP laminate placed in its dominant direction is highly unlikely. This is due to the fact that the failure typically occurs at the bond with the concrete surface, long before the CFRP reaches its ultimate strength

3.3.3 Shear Strength of the Epoxy

Another possible failure is the shearing of the epoxy surface with the surface of the beam. This mode of failure is unlikely due to the fact that the typical failure of the bond between the epoxy and the surface of the concrete takes place first. Another critical consideration is surface preparation. It cannot be stressed enough that the surface must be clean and free of all particles in order to avoid premature bond failure with the concrete surface. (11) (12)

3.3.4 Strain Capacity of Concrete is Reached

ACI limits the amount of strain in concrete to .003 in their design procedure. If the strain levels in the concrete reach a value greater than 0.004, the concrete will experience a loss of aggregate interlock causing it to crack and move resulting in the complete collapse of the element. (1) This crushing action represents brittle failure, which a design engineer needs to avoid. The failure mode is similar to that of an over-reinforced section where the crushing of the concrete occurs before the steel yields representing a catastrophic failure that occurs suddenly without warning.

3.4 Discussion of Beam Behavior and Failure Mode

3.4.1 One-Point Loading

Figure 3.7 Failure of control beam 1-1

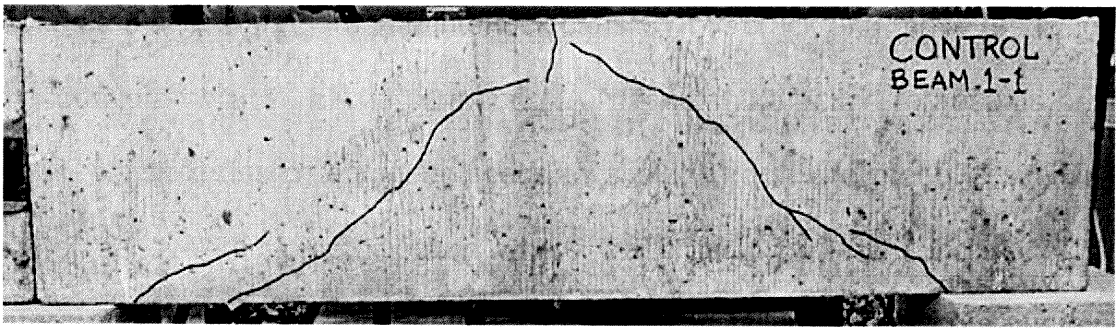

3.4.1.1 Control Beam 1-1. The nomenclature used for the beam testing is simple with the first number (either a one or two) standing for the loading condition and the second number representing the orientation of the CFRP laminate on the beam. The first beam tested was control beam 1-1, which failed in shear-compression. (Figure 3.7). As the beam was loaded beyond 16 kips, a

small crack developed directly under the load followed by flexural-shear cracks developing at each of the supports. These flexural-shear cracks developed at a forty-five degree angle between the load and the supports. Once the load reached its maximum of 21.2 kips, the flexural-shear cracks from the support connected with the crack under the load, resulting in shear-compression failure with the load dropping to 20 kips. At this point, the experiment was halted so that the beam could be used in future experiments where it could be repaired and re-tested.

3.4.1.2 Beam 1-2 Mid-Strip CFRP Location. The next beam tested was beam 1-2 with the CFRP laminate attached at the neutral axis, as pictured in Figure 3.8. The mode of failure for the beam was shear-compression failure similar to the control beam. As the load on beam increased past 17 kips, the first flexural-shear crack formed below the CFRP laminate near the right support. This crack formed at a forty-five degree angle with respect to the load and extended toward the load location as the load increased. At the ultimate load of 22.0 kips, the crack reached the load location and the beam failed suddenly with the load dropping 17.0 kips.

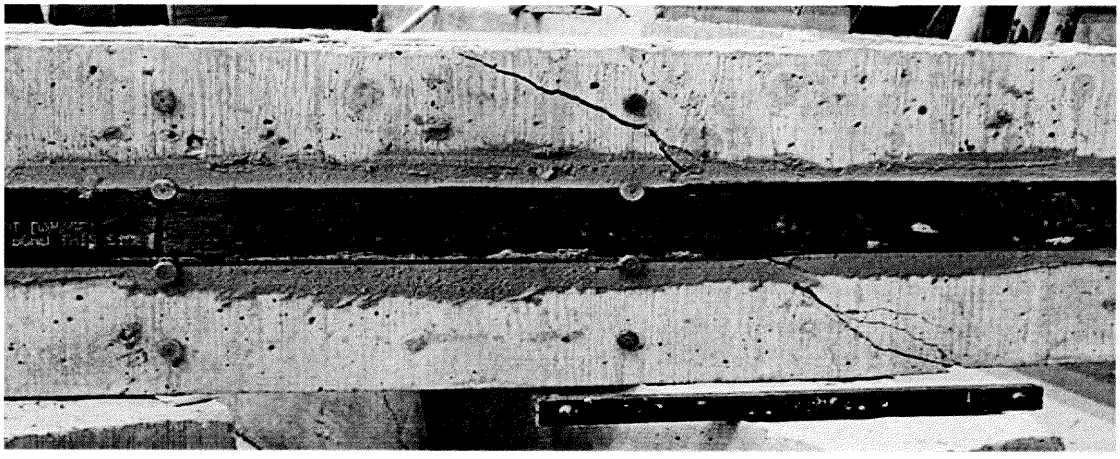

Figure 3.8 Failure of beam 1-2 with mid-strip CFRP location

3.4.1.3 Beam 1-3 90 Degree Aligned CFRP. Beam 1-3 with the ninety-degree aligned CFRP laminates with respect to the neutral axis of the beam failed in shear after the CFRP laminate debonded from the beam by shearing the surface of the concrete. During the testing procedure the first small flexural-shear crack appeared in the beam at 25 kips near the middle of the span on the tension side of the beam. As the load increased, more flexural cracks developed and small shear cracks develop at the supports between the CFRP laminates. As the load reaches a maximum of 37.8 kips, the flexural cracks continued to grow larger and the deflection increased without any further load increase. At this point, there was a loud popping sound as the bond between the CFRP and the concrete surface ruptured. The load dropped dramatically from 37.0 kips to 6.0 kips resulting in an explosive failure causing large pieces of concrete from the beam to scatter. Two CFRP laminates located third and fourth from the left support became completely dislodged. (Pictured in Figure 3.9) Figure 3.10 is a picture of the reverse side of

the beam showing that only the second CFRP laminate from the left support became dislodged.

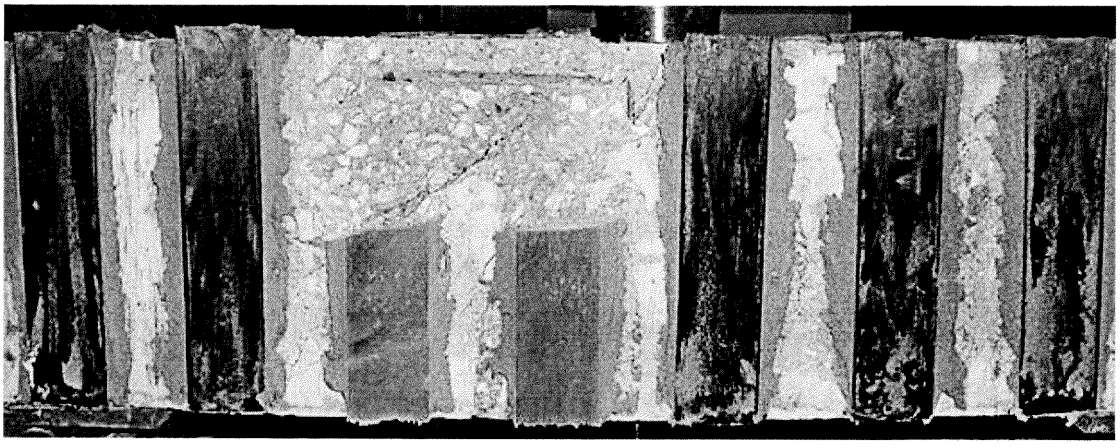

Figure 3.9 Failure of beam 1-3 with 90 degree aligned CFRP

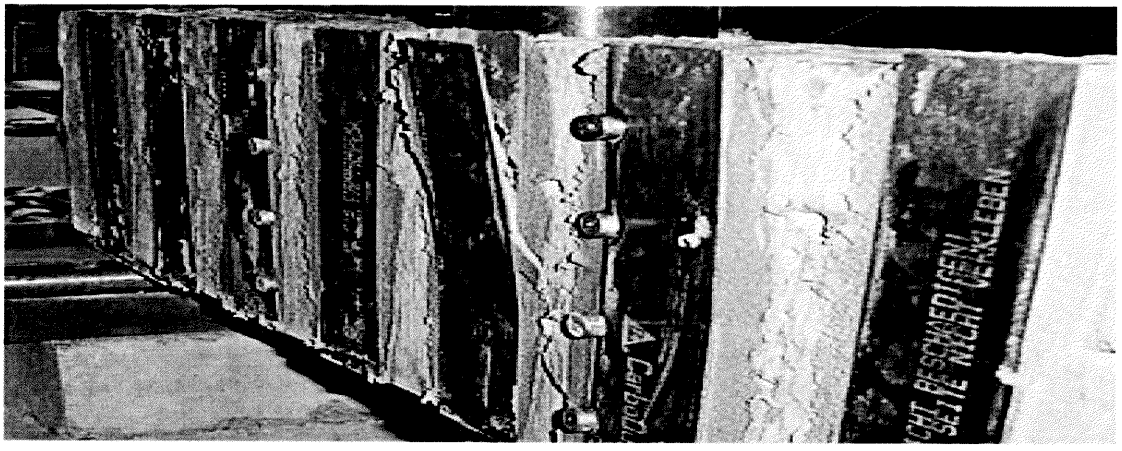

Figure 3.10 Beam 1-3 failure reverse side photo

3.4.1.4 Beam 1-4 45 Degree Aligned CFRP. Beam 1-4, with the forty-five degree aligned CFRP laminates (with respect to the neutral axis of the beam), failed in shear after the CFRP laminate debonded from the beam by shearing the surface of the concrete. As the beam was loaded, local failure was observed directly under the load at about 20 kips with no other crack development until

approximately 28 kips. At this point, flexural cracks began to form directly under the load on the tension side of the beam, and as the load increased these cracks continued up into the compression zone of the beam. During this period, shear cracks began to form perpendicularly to the CFRP laminates as pictured in Figure 3.11. As the load increased to a maximum of 45.9 kips the flexural cracks were approaching the neutral axis of the beam when the bonding between the CFRP laminate and the concrete surface yielded. This action was accompanied by a loud popping sound with the CFRP delaminating from the concrete with explosive force. The entire section located under the load fractured with large portions of concrete being dislodged and falling off. Figure 3.12 shows that the region from the load to the right support has become completely dislodged from the beam.

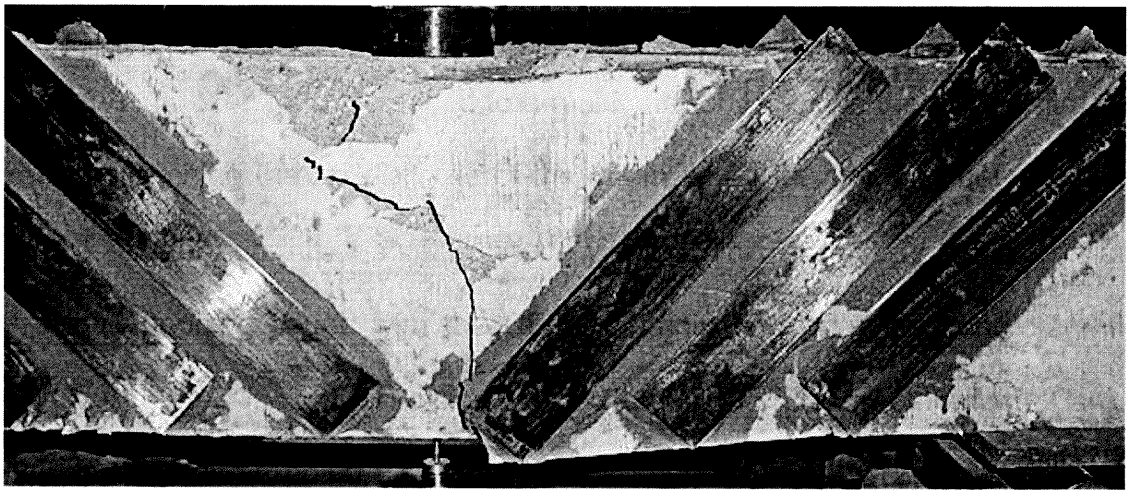

Figure 3.11 Failure of beam 1-4 with 45 degree aligned CFRP

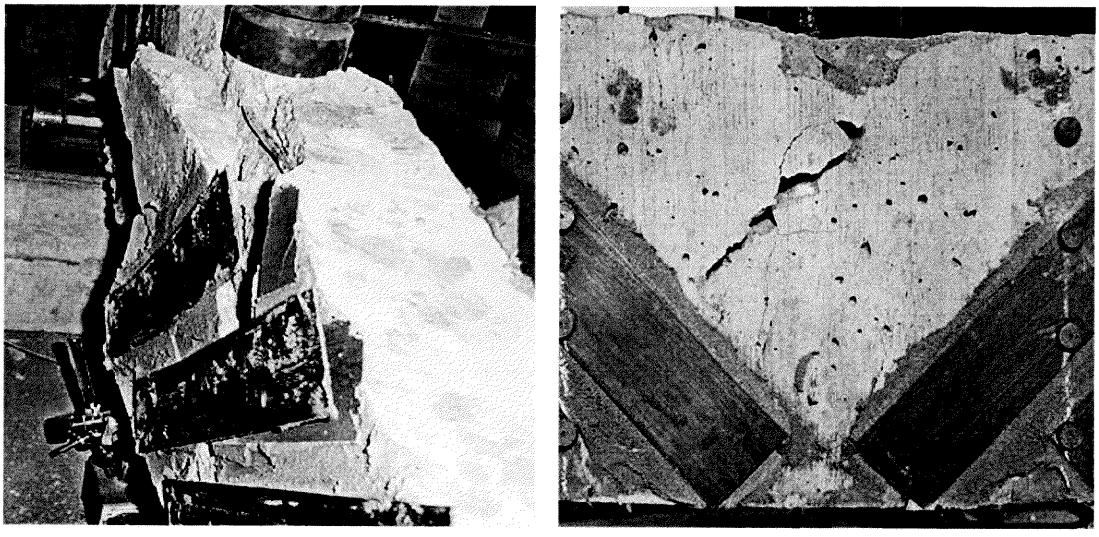

Figure 3.12 Beam 1-4 failure reverse and top view photo

3.4.2 Two-Point Loading

3.4.2.1 Control Beam 2-1. The first two-point loading test was conducted on control beam 2-1, which failed in shear-compression. (Figure 3.13). As the beam was loaded past 9.0 kips, a small crack formed directly under the left loading point. At 18 kips a small flexural shear crack developed at the right support and continued to lengthen as the load was increased. At 24 kips a flexural shear crack developed at the left support, while the crack at the right support reached the neutral axis of the beam. These cracks developed at a forty-five degree angle between the load and the supports. Once the load reached its maximum of 32.5 kips, the crack from the right support connected with the crack under the load resulting in the load dropping to 30.0 kips. The experiment was terminated after the load dropped to 20 kips.

Figure 3.13 Failure of control beam 2-1

3.4.2.2 Beam 2-2 Mid-Strip CFRP Location. The next beam tested was beam 2-2 with the CFRP laminate attached at the neutral axis as pictured in Figure 3.14. The mode of failure for the beam was shear-compression. As the load on the beam increased past 24 kips, the first flexural shear crack formed below the CFRP laminate near the right support. This crack formed at a forty-five degree angle with respect to the load and extended toward the load location as the load increased. At an ultimate load of 45.9 kips, the crack reached the location of the load and the beam suddenly failed with the load dropping to 37.0 kips. As the load was maintained and the deflection increased, the CFRP laminate began to split apart and the experiment was terminated after the deflection point reached four inches.

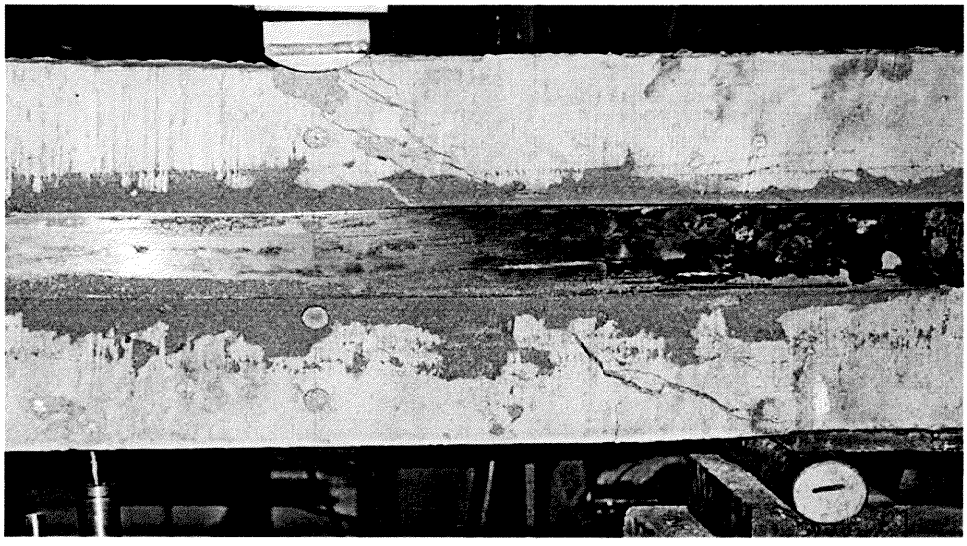

Figure 3.14 Failure of beam 2-2 with mid-strip CFRP location

3.4.2.3 Beam 2-3 90 Degree Aligned CFRP. Beam 2-3 with the ninety-degree aligned CFRP laminates (with respect to the neutral axis of the beam) failed in shear after the CFRP laminate debonded from the beam by shearing the surface of the concrete. During the testing procedure the first small flexural crack appeared in the beam at 28 kips near the middle of the span on the tension side of the beam. As the load increased, more flexural cracks developed and small shear cracks developed at the supports between the CFRP laminates. As the load reached a maximum of 46.7 kips, there was a loud popping sound as the bond between the CFRP and the concrete surface ruptured. The load dropped dramatically from 46.7 kips to 31.0 kips resulting in the three CFRP laminates at the left support to debond from the concrete surface causing the beam to fail in shear. Pictured in Figure 3.15 are the three CFRP laminates that debonded at failure. The entire portion of the laminate in the picture is hanging by a thread

and could easily be pulled off supporting the observation that the mode of failure occurred between the CFRP laminate and the concrete surface. Figure 3.16 shows the flexural shear cracks that formed between the CFRP laminate strips.

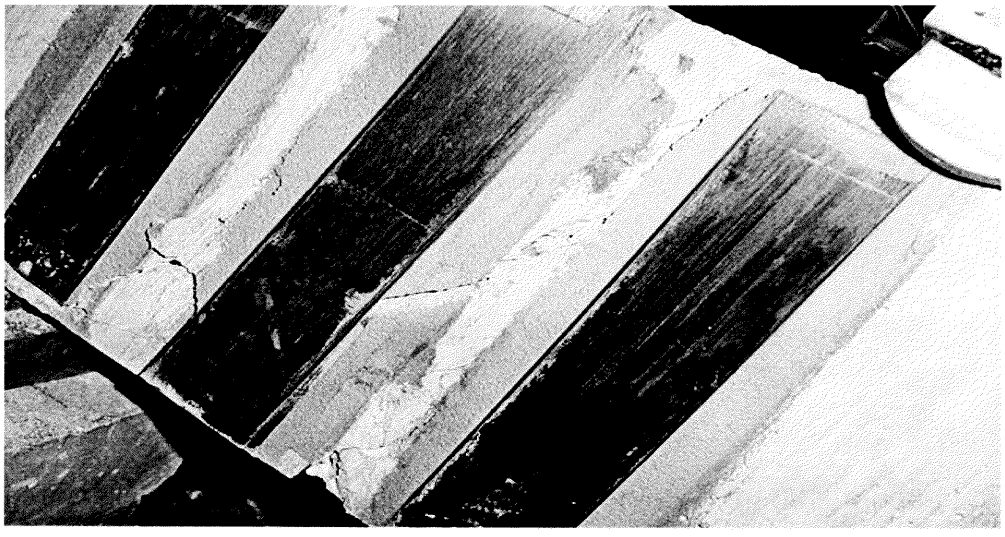

Figure 3.15 Failure of beam 2-3 with 90 degree aligned CFRP at left support

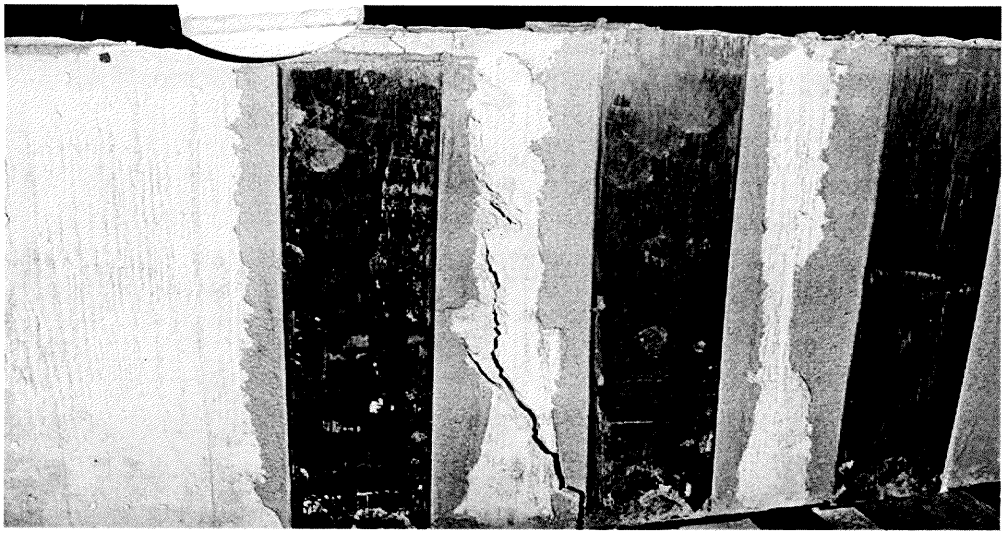

Figure 3.16 Failure of beam 2-3 with 90 degree aligned CFRP at right support

3.4.2.4 Beam 2-4 45 Degree Aligned CFRP. Beam 2-4 with the forty-five degree aligned CFRP laminates (with respect to the neutral axis of the beam) failed in shear after the CFRP laminate debonded from the beam by shearing the surface of the concrete. At 12 kips, local failure was observed directly under both of the loading points. As the load reached 30 kips, flexure-shear cracks began to develop directly under the loads on the tension side of the beam. The cracks propagated in the direction of the load location as the load increased in magnitude. When the load increased to approximately 40 kips, shear cracks began to form perpendicularly to the CFRP laminates, as pictured in Figure 3.17. As the load increased to a maximum of 54.1 kips, the flexural cracks passed the neutral axis of the beam and connected with the shear cracks that had formed perpendicularly to the CFRP laminate. At this point, there was a loud popping sound as the CFRP delaminated from the surface of the concrete. The entire concrete surface located from the support to the load location point fractured and separated from the beam. Figure 3.17 and Figure 3.18 show that the failure condition occurred at both supports.

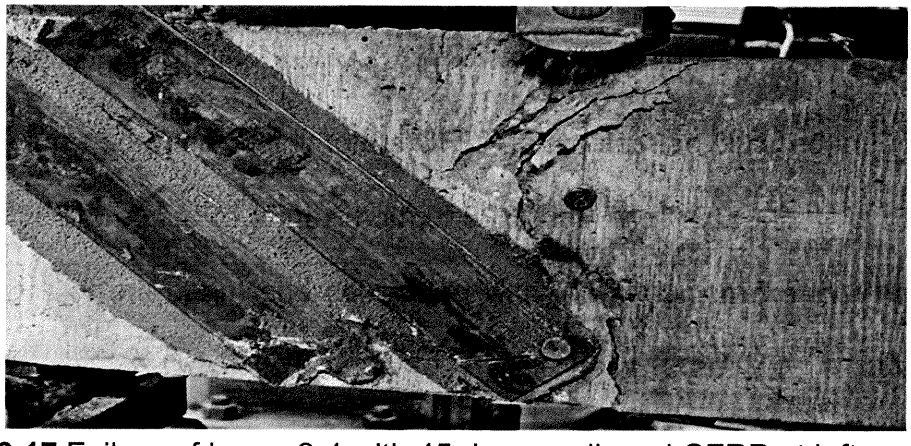

Figure 3.17 Failure of beam 2-4 with 45 degree aligned CFRP at left support

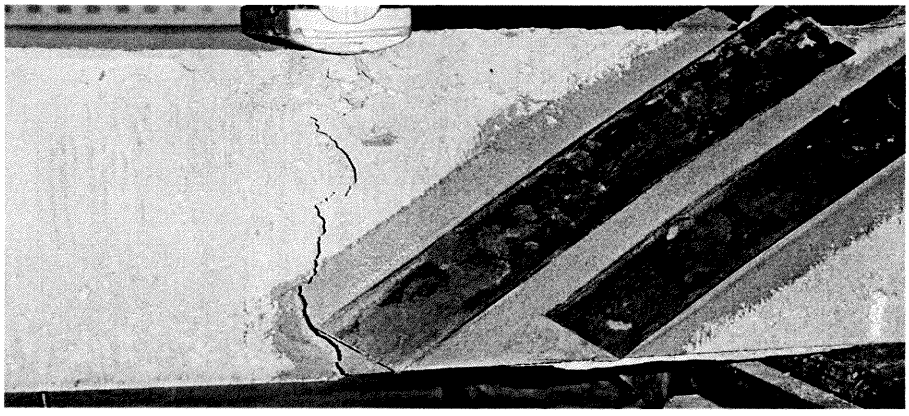

Figure 3.18 Failure of beam 2-4 with 45 degree aligned CFRP at right support

3.5 Test Results

3.5.1 One-Point Loading

A summary of the one-point loading results is provided in Table 3.1. Included in this table are the values for the ultimate load and deflection, the CFRP shear capacity increase and the final failure mode of the beam. Figure 3.19 combines all four of the beam load deflection curves onto the same graph for easy comparison. The individual load deflection curves are located in the Appendix C, Individual Load Deflection Curves.

Table 3.1 Experimental results for one-point loading

Beam Number	Ultimate Load (lbs)	Deflection at Ultimate (in.)	CFRP Shear Capacity(lbs)	Mode of Failure
1-1	21199	.090872	—	Shear Compression
1-2	21999	.081659	800	Shear Compression
1-3	37801	.129618	16602	Strip Delamination
1-4	43499	.205680	22300	Strip Delamination

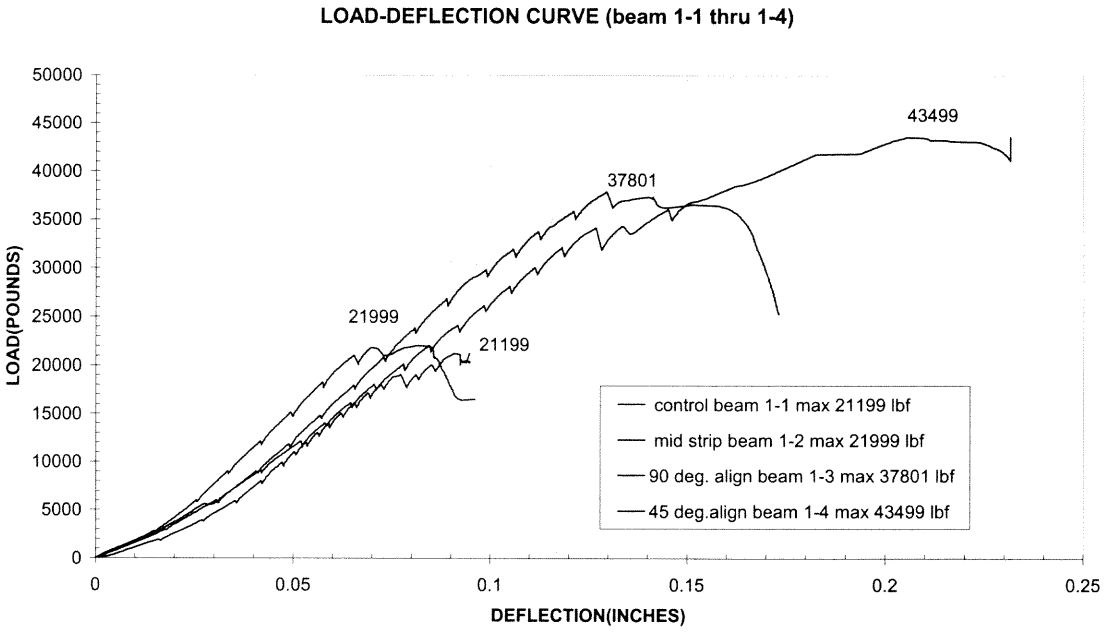

Figure 3.19 Combined load deflection curve for one-point loading

3.5.1.1 Strength. It can be observed from Table 3.1 and Figure 3.19 that the externally bonded CFRP laminate increased the load carrying capacity of the reinforced concrete deep beams tested. Since the mode of failure was shear in all four beams tested, a direct connection can be made between the arrangement of the CFRP laminate and the increase in shear capacity of the deep beams. The beam with the forty-five degree aligned CFRP laminate experienced a 22.5 kip increase in ultimate shear capacity over the control beam. This was the largest increase in shear capacity followed by the ninety-degree aligned CFRP laminate, which contributed a 16.6 kip increase in shear capacity. The zero degree aligned CFRP laminate increased the shear strength the least, with only an 800 pound increase over the control beam.

3.5.1.2 Ductility. Referring to Table 3.1, the ultimate deflection at the time of failure for the bonded CFRP laminate was significantly increased over the control beam for the forty-five and ninety degree CFRP orientations. The forty-five degree aligned CFRP laminate beam increased in deflection by a hundred and twenty percent, while the ninety-degree aligned CFRP laminate beam increased in deflection by forty percent over the control beam. The beam with the mid-strip CFRP laminate location did not experience any increase in deflection over the control beam; in fact, it experienced a ten- percent loss. The increase in deflection for the bonded forty-five and ninety-degree aligned CFRP laminate over the control beam indicates that not only is the shear capacity of the beam increased, but also its serviceability.

By measuring and recording the strain and load on the beam during the experiment, the longitudinal curvature was determined and compared to the control beam. If the radius of curvature (the inverse of the longitudinal curvature) for the control beam is longer than the radius of curvature for the bonded CFRP laminate beam, it can be surmised that the CFRP bonded laminate increases the ductility of the beam. By plotting the moment-curvature curve for all four of the beams tested on the same graph, it can be observed which CFRP alignment arrangement has the most increase in ductility. The forty-five and ninety-degree aligned CFRP laminate beams experienced a significant increase in ductility over the control beam. The areas under the moment-curvature curve for the forty-five and ninety-degree aligned CFRP laminate is more than double that of the control

beam area. (Figure 3.20) Also see Appendix D, Individual Moment-Curvature curves

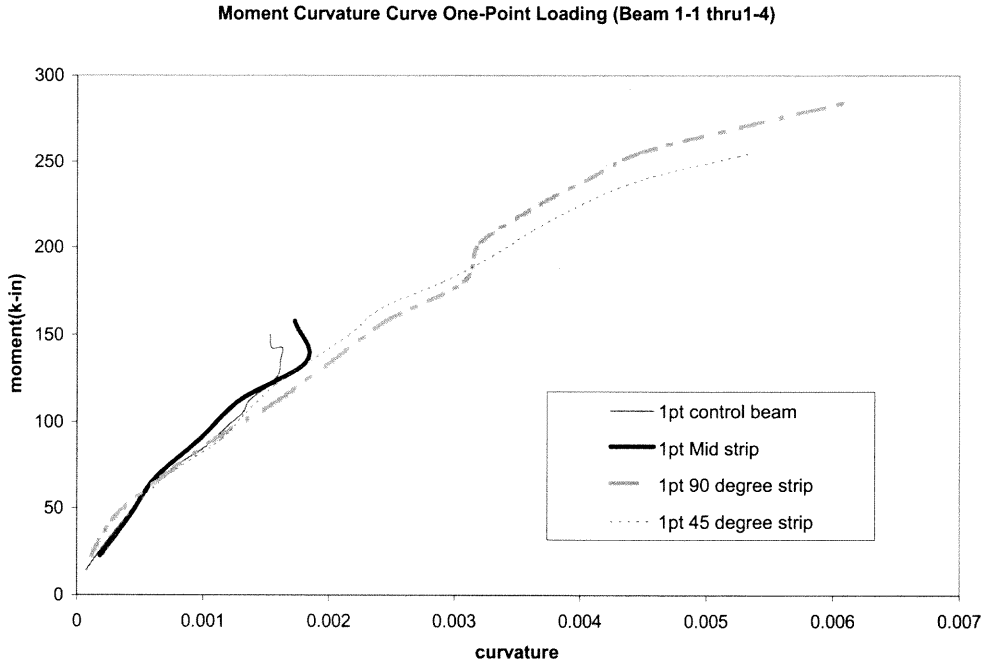

Figure 3.20 Moment-curvature for one-point loading condition

3.5.2 Two-Point Loading

A summary of the two-point loading results is provided in Table 3. 2. Included in this table are the values for the ultimate load and deflection, the CFRP shear capacity increase and the final failure mode of the beam. Figure 3.21 combines all four of the beam load-deflection curves onto the same graph. The individual load deflection curves are located in the Appendix C, Individual Load Deflection Curves.

Table 3.2 Experimental results for two-point loading

Beam Number	Ultimate Load (lbs)	Deflection at Ultimate (in.)	CFRP Shear Capacity(lbs)	Mode of Failure
2-1	32502	.076493	—	Shear Compression
2-2	45900	.108075	13398	Shear Compression
2-3	46702	.122223	14200	Strip Delamination
2-4	54103	.109607	21601	Strip Delamination

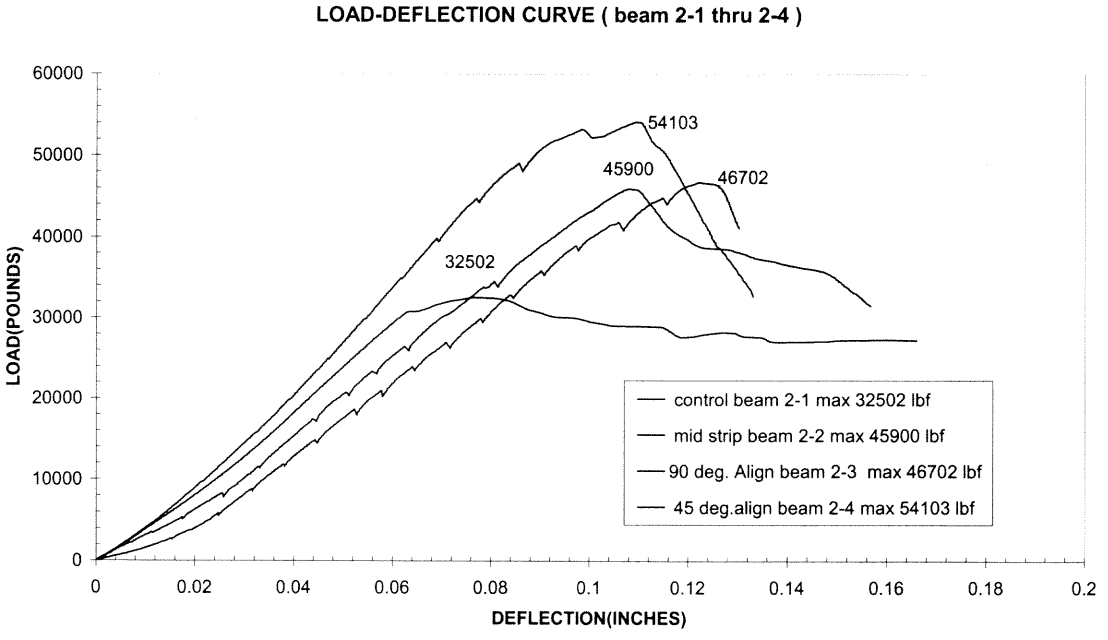

Figure 3.21 Combined load deflection curve for two-point loading

3.5.2.1 Strength. It can observed from Table 3.2 and Figure 3.21 that the externally bonded CFRP laminate increased the load carrying capacity of the reinforced concrete deep beams tested. Since the mode of failure was shear in

all four beams tested, a direct connection can be made between the arrangement of the CFRP laminate and the increase in shear capacity of the deep beams. The beam with the forty-five degree aligned CFRP laminate experienced the largest increase in shear capacity with a 21.6 kip increase in ultimate shear capacity over the control beam. The ninety and the zero degree aligned CFRP laminate contributed 14.2 kip and 13.3 kip, respectively to the shear capacity of the beam.

3.5.2.2 Ductility. Referring to Table 3.2 the ultimate deflection at the time of failure for the bonded CFRP laminate was significantly increased over the control beam for all the CFRP orientations. The beam with the ninety-degree aligned CFRP laminate increased in deflection by sixty percent. While the forty-five and zero degree aligned CFRP laminates increased in deflection by forty percent over the control beam. The increase in deflection for the bonded zero, forty-five, and ninety-degree aligned CFRP laminate over the control beam indicates that not only is the shear capacity of the beam increased, but also its serviceability.

By monitoring the strain in the beams during the experiment, the longitudinal curvature can be calculated and compared to the control beam. When the radius of curvature (the inverse of the longitudinal curvature) of the control beam is longer than the radius of curvature for the CFRP bonded beams, it can be surmised that the bonded CFRP laminate increases the ductility of the beam. By plotting the moment-curvature of all four beams on the same graph it can be observed that the zero, forty-five, and ninety-degree aligned CFRP laminate beams experienced a significant increase in ductility. (Figure 3.22)

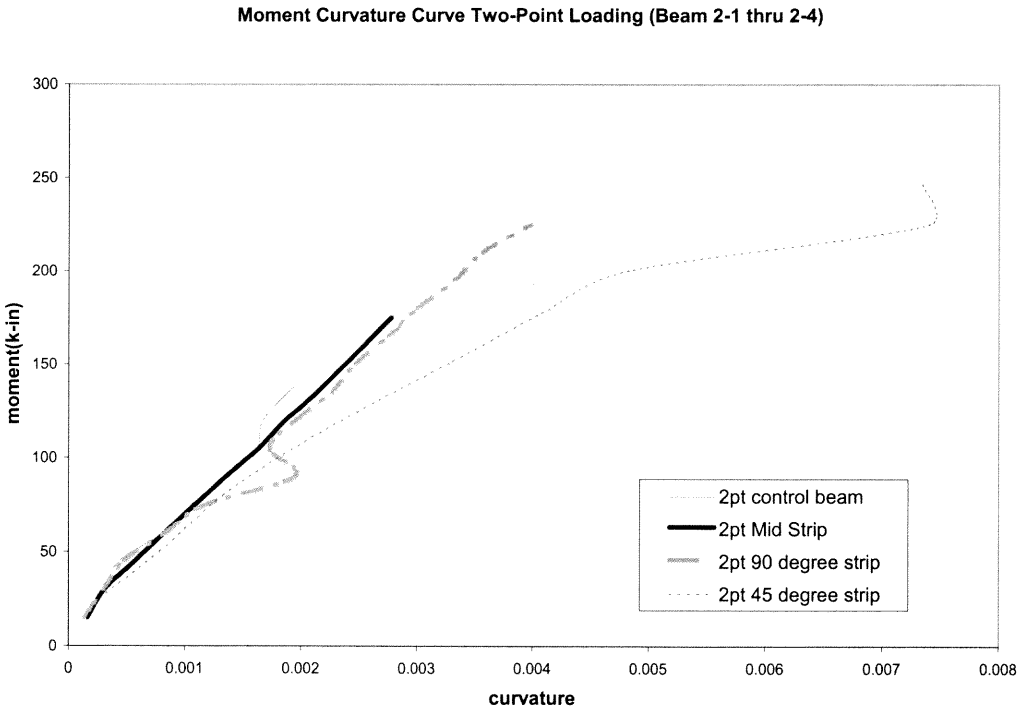

Figure 3.22 Moment–curvature curve for two-point loading condition

Chapter 4

SUMMARY AND CONCLUSION

This experiment investigated the behavior of reinforced concrete deep beams with shear deficiencies strengthened with different configurations of CFRP laminates. The test results indicate that the externally bonded CFRP laminates enhance the shear capacity of the deep beams tested. For the one-point loading condition the shear increase ranged from one hundred and five percent for the beam 1-4 to three and a half percent for beam 1-2. The two-point loading condition had shear increases that ranged from sixty-six percent for beam 2-4 to forty percent for beam 2-2.

The orientation of zero, forty-five, and ninety-degree aligned CFRP laminates were evaluated in two separate loading conditions. The forty-five degree aligned CFRP laminates for the one- and two-loading conditions increased the shear strength of the deep beam the largest amount. The ninety-degree configuration had the next largest increase in shear capacity with seventy-eight percent increase for the one-point loading and forty-four percent increase for the two-point loading condition. The zero degree aligned CFRP laminate for the one-point loading condition did not contribute a noticeable amount of shear strength with only a three percent increase. The zero-degree aligned CFRP laminate for the two-point loading condition, however, experienced a forty percent increase in shear strength, which was unexpected. In experiments by Khalifa and Nanni, “the zero degree aligned ply did not contribute to the shear strength of the test specimen” (3). A possible explanation for this result is that a

compressive arch formed during loading, which gave the beam an increased shear-carrying capacity. If this were the case, then the mode of failure could be changed from shear compression failure to arch-rib failure.

The externally bonded CFRP laminate improved the serviceability of most of the beams tested. The forty-five and ninety degree aligned CFRP laminate increased the serviceability of the beam the most. The deflection at the ultimate load increased by as much as one hundred and twenty percent in the case of beam 1-4. All the beams tested with the exception of beam 1-2 experienced a forty percent increase in deflection over their respective control beams.

The ductility of the beams tested also increased with the externally bonded CFRP laminates. The forty-five and ninety degree aligned CFRP laminate increased the area under the moment-curvature curve by as much as two times that of the control beam. In all the experiments conducted, with the exception of beam 1-2 the ductility of the deep beam was increased by externally bonded CFRP laminate.

The type of shear failure experienced by both control beams was a bit of a disappointment. It was hoped that when the beams were loaded a compressive arch would form giving the beam a large amount of reserve shear capacity. Instead the failure observed was typical shear compression failure, with only beam 2-2 demonstrating any unusual shear caring capacity. This could be explained by the fact that deep beam behavior is influenced by the height to width ratio of the beam. The height of the beam for this experiment may not have been large enough for the compression arch to develop. The scale of the beam

tested in this experiment may also have had an influence on the shear behavior observed. The beam tested represents a quarter size of an actual ACI classified deep beam. The shear behavior may be different for a half-size or full-size beam based on the dimensions used for the beam tested.

The experiments performed on the deep beams introduced in this thesis should only be considered a starting point for a better understanding of the strengthening effect of CFRP laminates in shear. Many more tests must be conducted on full-sized deep beams in order to understand exactly how the failure mechanisms are influenced. The condition of the structure must be completely understood before CFRP strengthening system is applied. If the CFRP laminate is installed incorrectly, the mode of failure could change from ductile bending failure to brittle compressive failure. This must be avoided at all cost, for the safety of the public is the engineer's number one priority. However, with this in mind the experiments conducted demonstrate that reinforced concrete deep beams can be strengthened in shear.

APPENDIX A

ACI REINFORCED CONCRETE DEEP BEAM DESIGN

In this Appendix, the ACI flexural strength and shear capacity of the deep beam is calculated by hand.

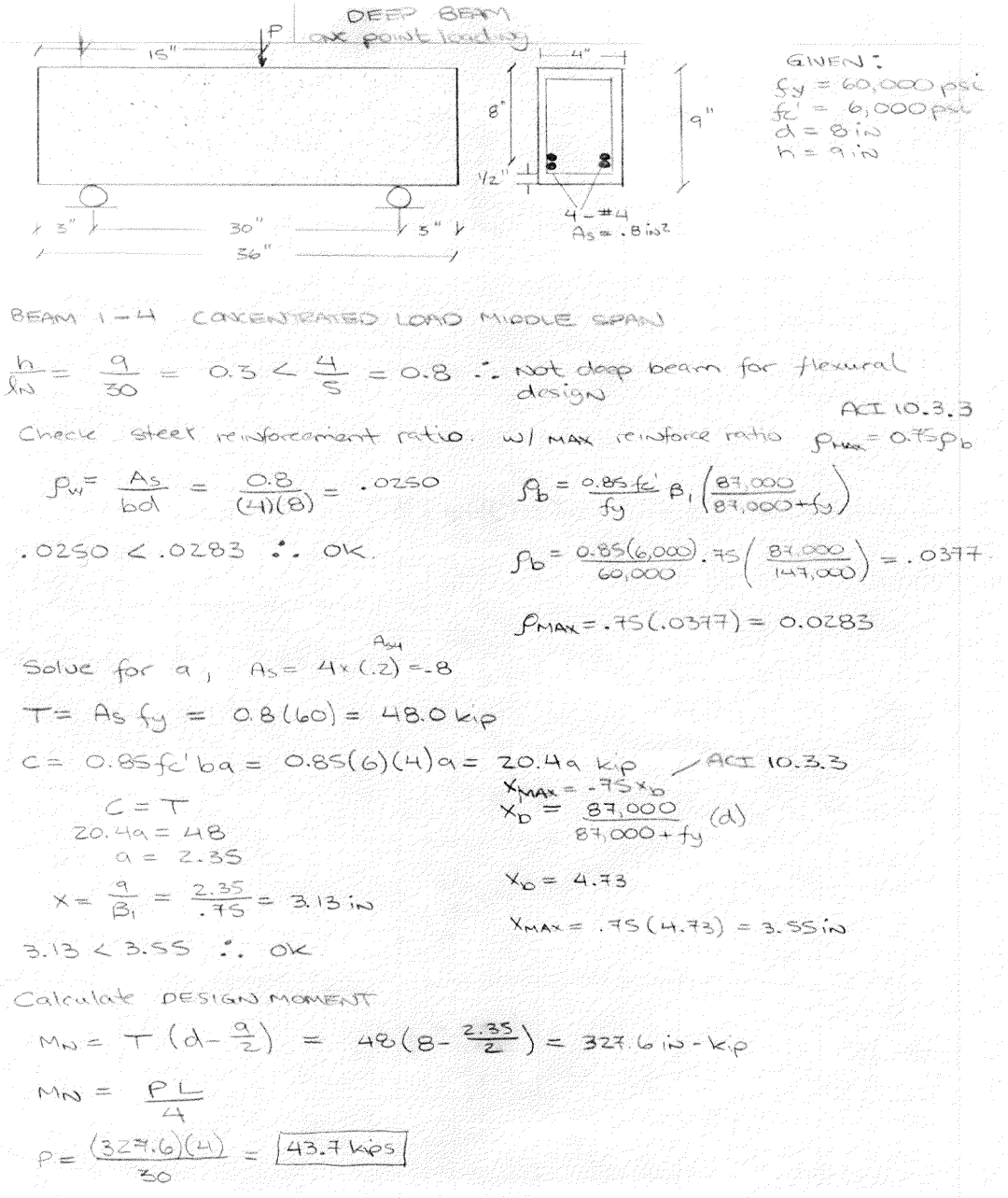

Figure A.1 Deep beam calculations one-point loading

DEEP BEAM
one point loading

Shear strength of Concrete V_c
ACI - 11.8 classifies deep beam as having a $L_N/d < 5$
For concentrated load mid span $\frac{L_P}{d}$ of 5 & $\frac{a}{d} = 2.5$.

GIVEN $a = 15''$
$d = 8'' = .667\,ft$ $\quad \frac{a}{d} = \frac{15}{8} = 1.88 < 2.5 \quad \therefore$ DEEP BEAM

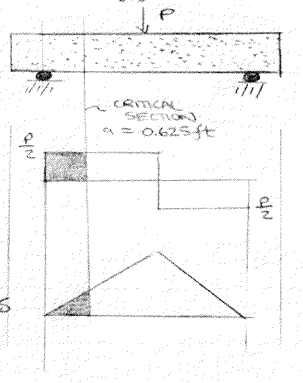

LOCA. CRITICAL SECTION

$0.5a = \frac{0.5(15)}{12} = .625\,ft$

Multiplier upper limit

$\left(3.5 - 2.5\frac{M_u}{V_u d}\right) \leq 2.5$

$\left(3.5 - 2.5\frac{.625(12)}{8}\right) = 1.156$

$V_u = \frac{P}{2}$

$M_u = \frac{P}{2}.625$

SHEAR STRENGTH V_c

$V_c = \left(3.5 - 2.5\frac{M_u}{V_u d}\right)\left(1.9\sqrt{f_c'} + 2500\,\rho_w \frac{V_u d}{M_u}\right) b_w d$ ACI 11-30

$V_c = (1.156)\left[1.9\sqrt{6000} + 2500(.0250)\frac{.667}{.625}\right](4)(8)$

$V_c = 7,910.4$

$P = V_c(2) = (7,910.4)(2) = 15.8\,kips$

Figure A.2 Deep beam calculations one-point loading continued

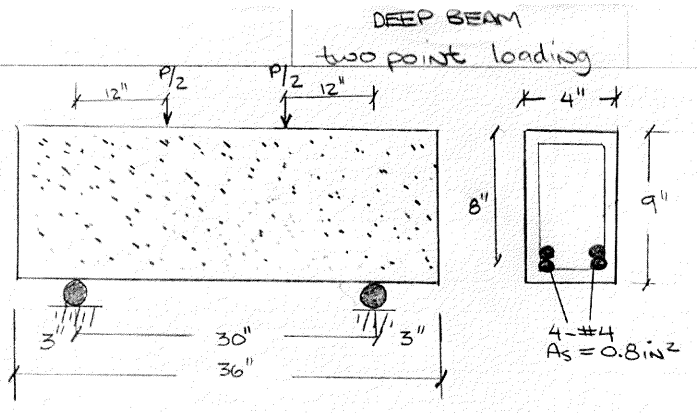

GIVEN:
$f_y = 60{,}000$ psi
$f_c' = 6{,}000$ psi
$d = 8$ in
$h = 9$ in

BEAM S-8 TWO POINT LOADING

PREVIOUS CALC.

$$\rho_w = \frac{A_s}{bd} = .0250$$

$$T = A_s f_y = 48 \text{ kip}$$

$$M_N = T\left(d - \frac{a}{2}\right) = 327.6 \text{ in-kip}$$

$$M_N = \frac{P(12)}{2} = 327.6$$

$$P = \boxed{54.6} \text{ kips}$$

SHEAR STRENGTH OF CONCRETE V_c.

GIVEN $a = 12"$, $d = 8"$ $\quad \frac{a}{d} = \frac{12}{8} = 1.5 < 2.5 \therefore$ DEEP BEAM IN SHEAR

LOCA. CRITICAL SECTION

$$0.5a = \frac{0.5(12)}{12} = .50 \text{ ft}$$

MULTIPLIER UPPER LIMIT. $\left(3.5 - 2.5\frac{M_u}{V_u d}\right) \leq 2.5$

$$\left(3.5 - 2.5\frac{(.5)(12)}{8}\right) = 1.625$$

SHEAR STRENGTH V_c

$$V_c = \left(3.5 - 2.5\frac{M_u}{V_u d}\right)\left(1.9\sqrt{f_c'} + 2500\rho_w \frac{V_u d}{M_u}\right) b_w d$$

$$V_c = 1.625\left[1.9\sqrt{6000} + 2500(.0250)\frac{.667}{.5}\right](4)(8)$$

$$V_c = 11{,}988$$

$$V_c = V_c(2) = 23.97 \approx 24.0 \text{ kips}$$

Figure A.3 Deep beam calculations two-point loading

APPENDIX B

CONCRETE MIX DESIGN AND TEST CYLINDER STRESS STRAIN CURVES

This Appendix contains the computer printout of the mix specifications and proportions as well as the stress stain curves for the test cylinders.

This program calculates a CONCRETE MIX DESIGN based on the ABSOLUTE VOLUME METHOD as presented in ACI 211.1. The user needs to know the required SLUMP and STRENGTH, MAX AGGREGATE SIZE and FINENESS MODULUS. Additionally, the SATURATED SURFACE DRYED SPECIFIC GRAVITIES of the COARSE and FINE AGGREGATES are needed as well as the %MOISTURE and %ABSORBANCE for both aggregates. Intermediate calculations are provided to aid in understanding the ABSOLUTE VOLUME METHOD.

Required Slump (consult Table 6.3.1) 3-4 inches □Required Strength 5000 psi □Fineness Modulus of Fine Aggregate 2.79

Maximum Coarse Aggregate Size 3/4 inch

Estimated Water (per cubic yd.) from Tab. 6.3.3 $EW := 340$ lbs

Estimated Entrapped Air % from Tab. 6.3.3 $A := 2$ %

Water/Cement Ratio from Tab. 6.3.4a $r := 0.48$

Dry Rodded Unit Weight of Coarse Aggregate $DRUW := 103$ lbs

Volume of Coarse Aggregate per unit volume from Tab. 6.3.6 $DRV := 0.62$ cu.ft.

Specific Gravity of Coarse Aggregate $Csg := 2.65$

Specific Gravity of Fine Aggregate $Fsg := 2.55$

C A L C U L A T I O N S for ONE cubic ft.

$$W := \frac{EW}{27} \qquad VW := \frac{W}{62.4} \qquad VW = 0.202 \text{ cu.ft.}$$

$$VA := \frac{A}{100} \qquad VA = 0.02 \text{ cu.ft.}$$

$$C := \frac{W}{r} \qquad VC := \frac{C}{3.15 \cdot 62.4} \qquad VC = 0.133 \text{ cu.ft.}$$

$$WCA := DRUW \cdot DRV \qquad VCA := \frac{WCA}{Csg \cdot 62.4} \qquad VCA = 0.386 \text{ cu.ft.}$$

$$(VW + VA + VC + VCA) = 0.741 \text{ cu.ft.}$$

Calculation for Volume of Fine Aggregate applying Absolute Volume Method

$$VF := 1 - (VW + VA + VC + VCA) \qquad VF = 0.259 \text{ cu.ft.}$$

Weight of Fine Aggregate

$$WFA := VF \cdot Fsg \cdot 62.4 \qquad WFA = 41.139 \text{ lbs.}$$

Figure B.1 Concrete mix design

$$MCA := WCA \cdot \left(1 + \frac{CAMST}{100}\right) \qquad MCA = 63.86 \text{ lbs.}$$

$$MFA := WFA \cdot \left(1 + \frac{FAMST}{100}\right) \qquad MFA = 42.373 \text{ lbs.}$$

$$\left(WCA \cdot \frac{CAMST - CAABS}{100}\right) = -0.319 \text{ lbs.}$$

$$\left(WFA \cdot \frac{FAMST - FAABS}{100}\right) = 1.07 \text{ lbs.}$$

$$MW := W - \left(WCA \cdot \frac{CAMST - CAABS}{100}\right) - \left(WFA \cdot \frac{FAMST - FAABS}{100}\right) \qquad MW = 11.842 \text{ lbs.}$$

BATCH REQUIREMENTS

Total Volume Required $Q := 2.5$ cu.ft.

$Water := MW \cdot Q$	$Water = 29.606$	lbs.
$Cement := C \cdot Q$	$Cement = 65.586$	lbs.
$CoarseAggregate := MCA \cdot Q$	$CoarseAggregate = 159.65$	lbs.
$FineAggregate := MFA \cdot Q$	$FineAggregate = 105.932$	lbs.

Figure B.2 Concrete mix design continued

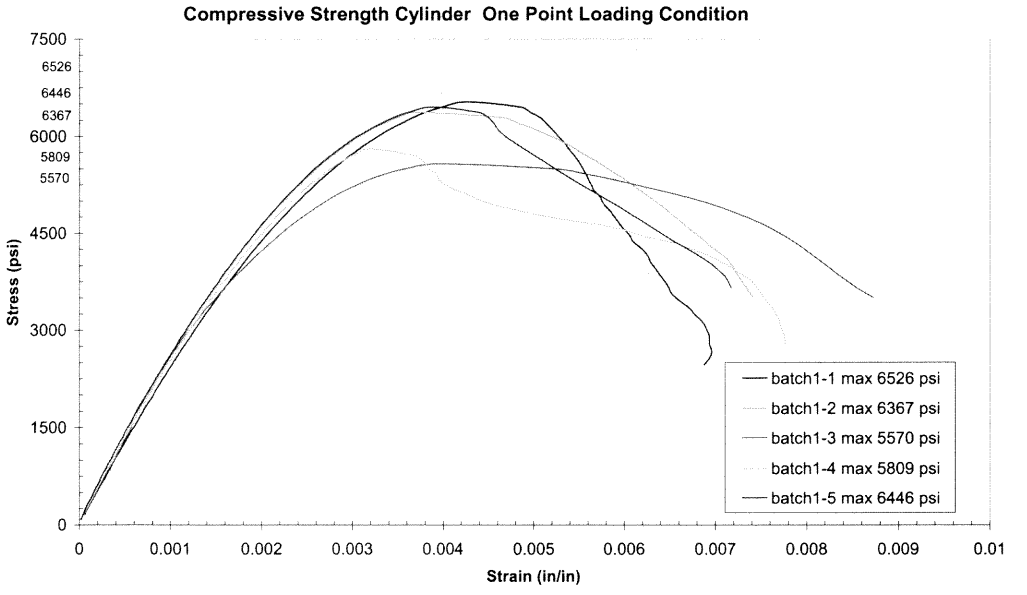

Figure B.3 Compressive strength of cylinders one-point loading

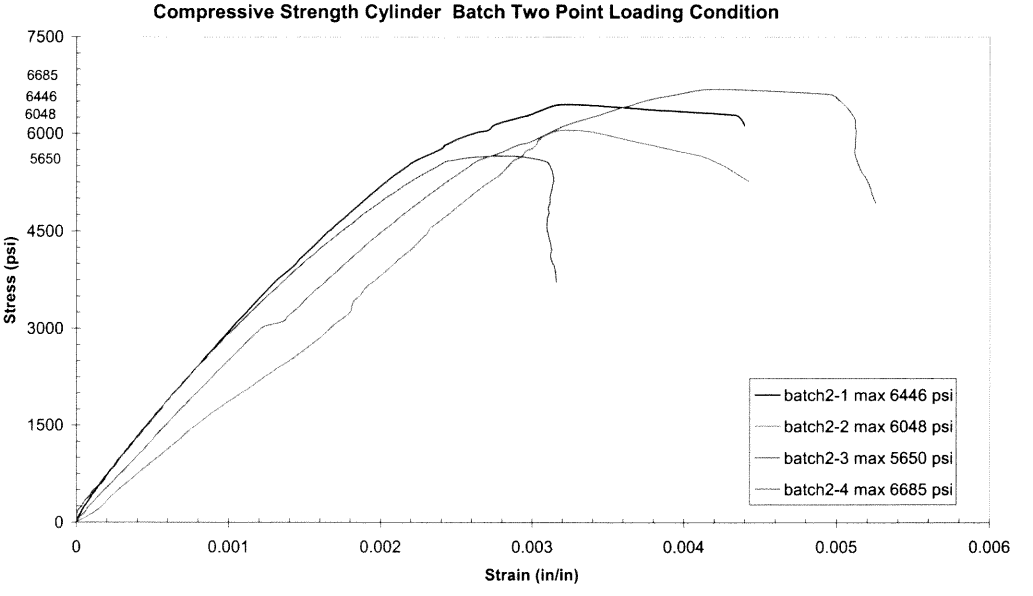

Figure B.4 Compressive strength of cylinders two-point loading

APPENDIX C

INDIVIDUAL LOAD DEFLECTION CURVES

The individual load deflection curves for the one- and two-point loading conditions are located in this Appendix.

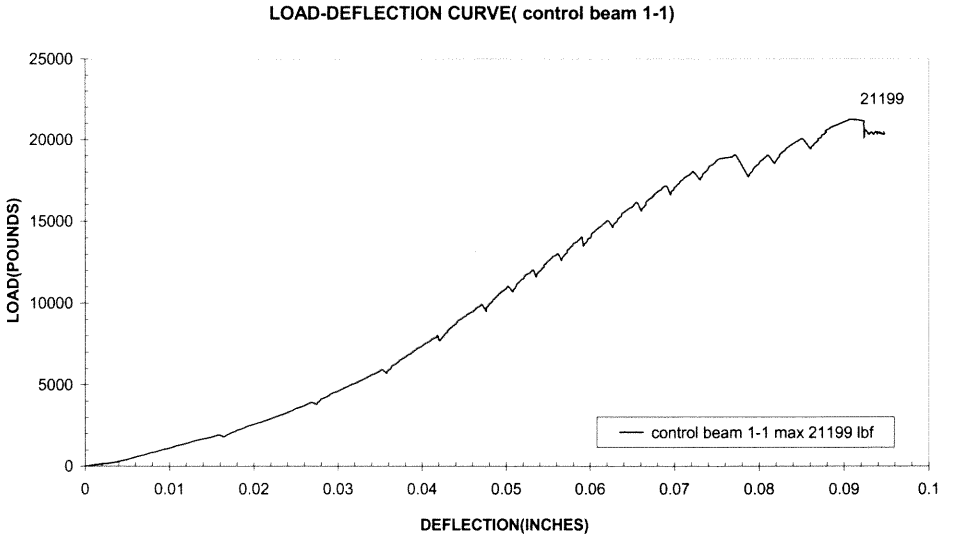

Figure C.1 Load deflection curve beam 1-1

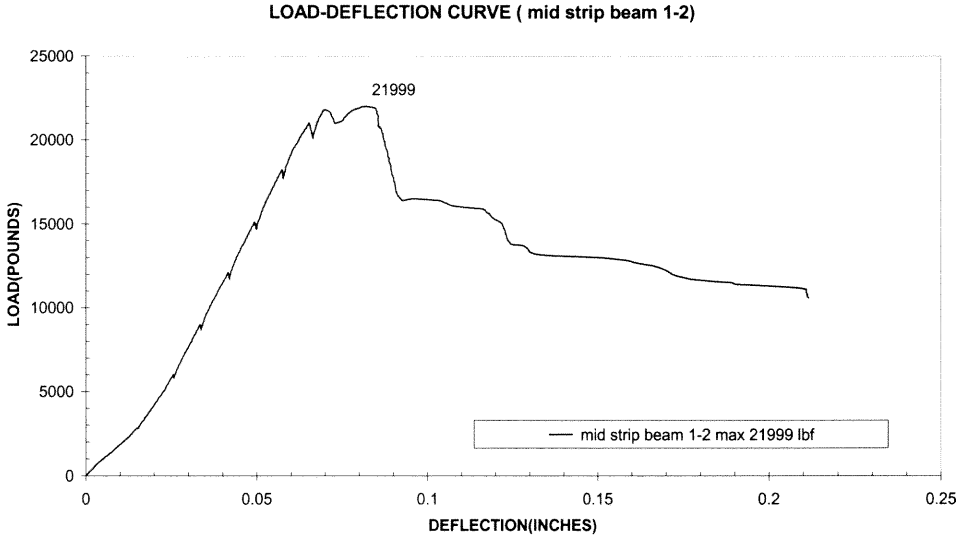

Figure C.2 Load deflection curve beam 1-2

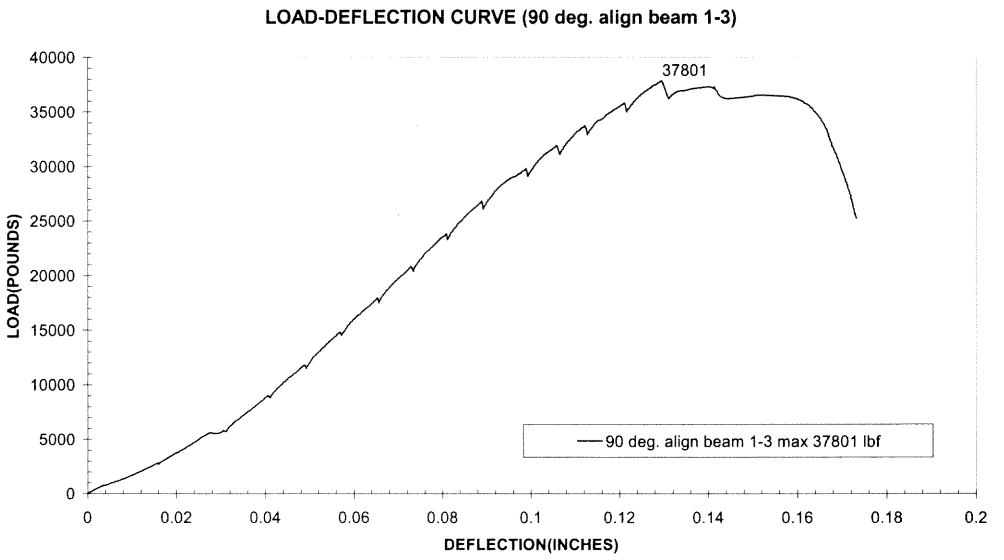

Figure C.3 Load deflection curve beam 1-3

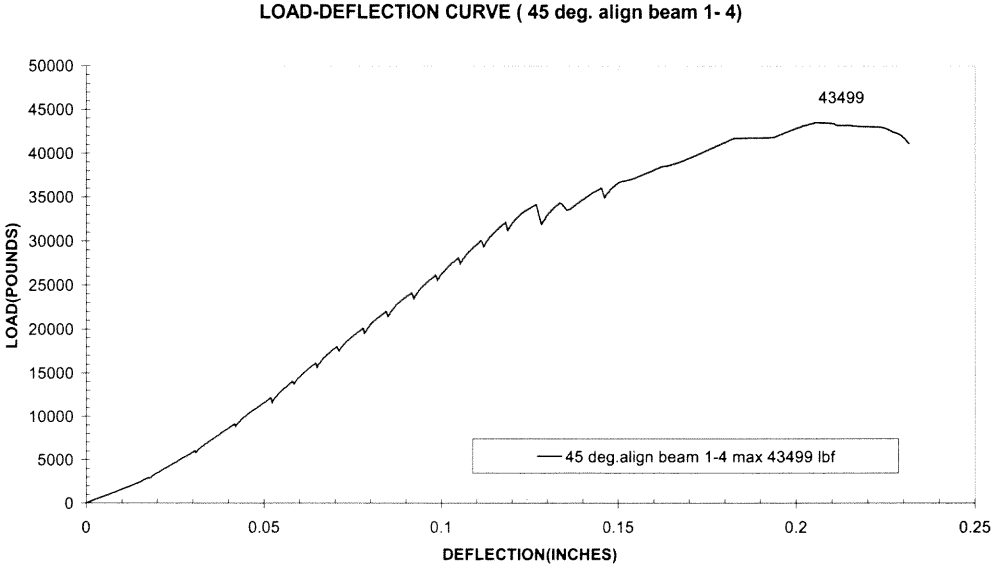

Figure C.4 Load deflection curve beam 1-4

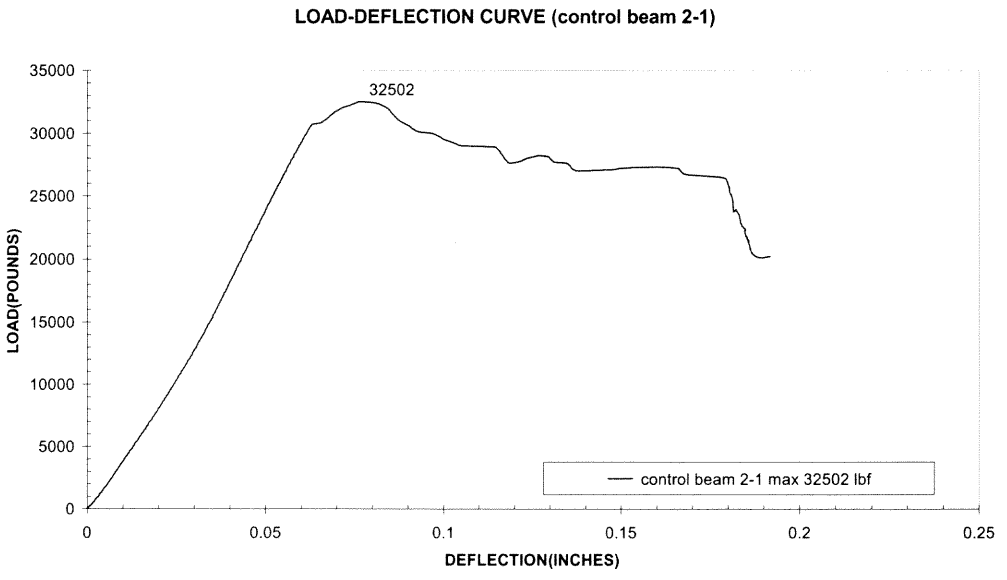

Figure C.5 Load deflection curve beam 2-1

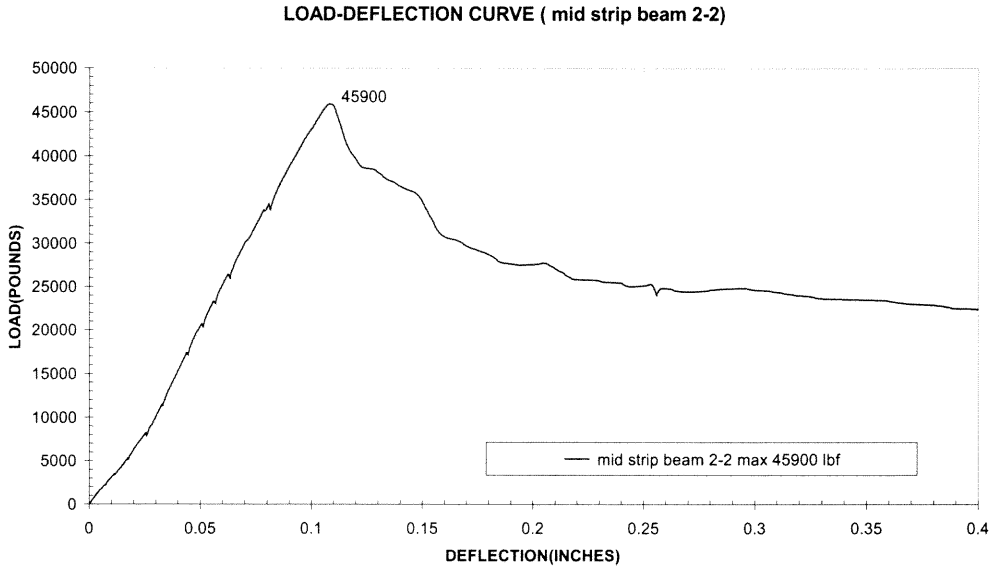

Figure C.6 Load deflection curve beam 2-2

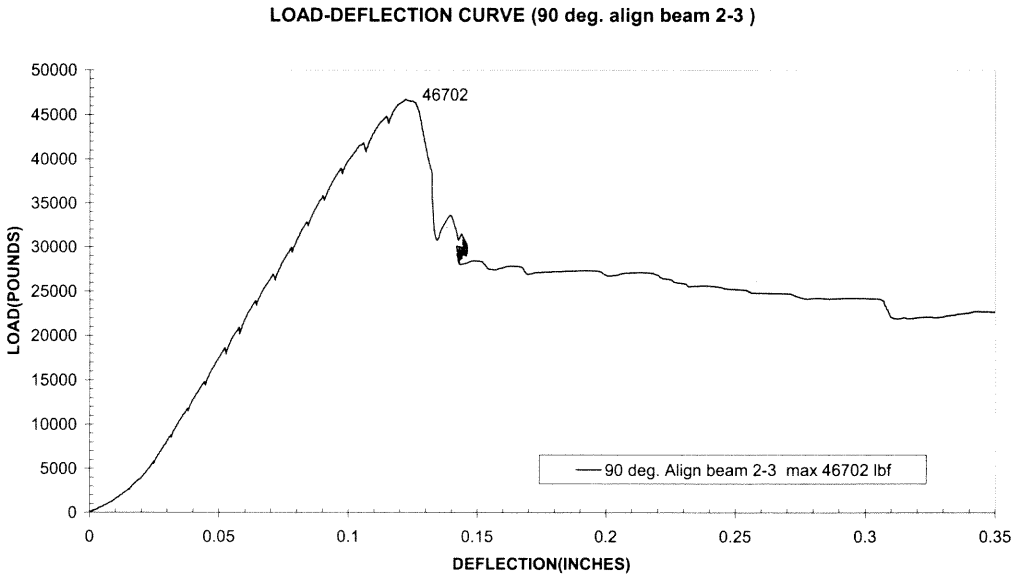

Figure C.7 Load deflection curve beam 2-3

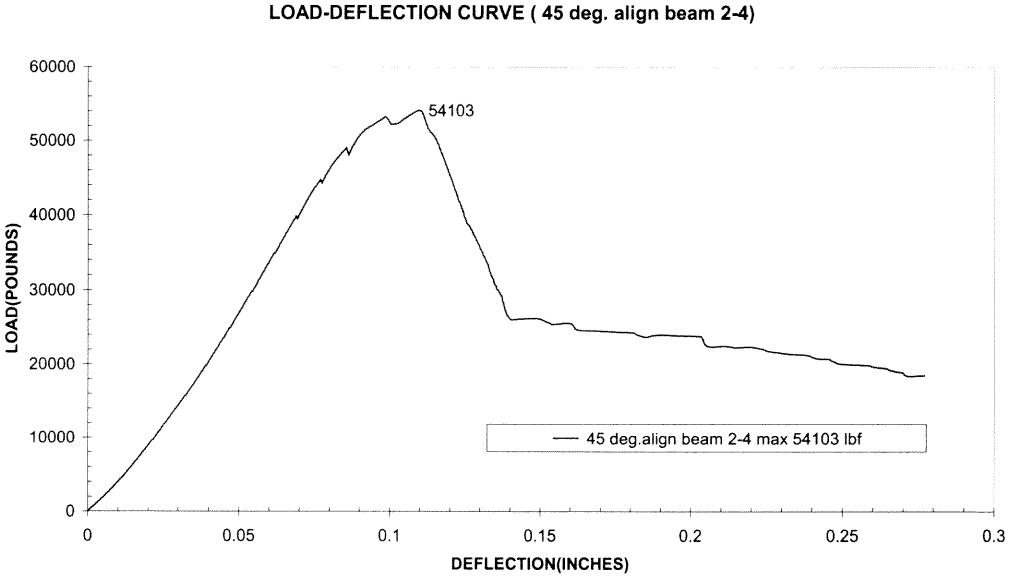

Figure C.8 Load deflection curve beam 2-4

APPENDIX D

INDIVIDUAL MOMENT-CUVATURE CURVES

In this Appendix the individual moment-curvature curves are displayed for both the one- and two-point loading conditions

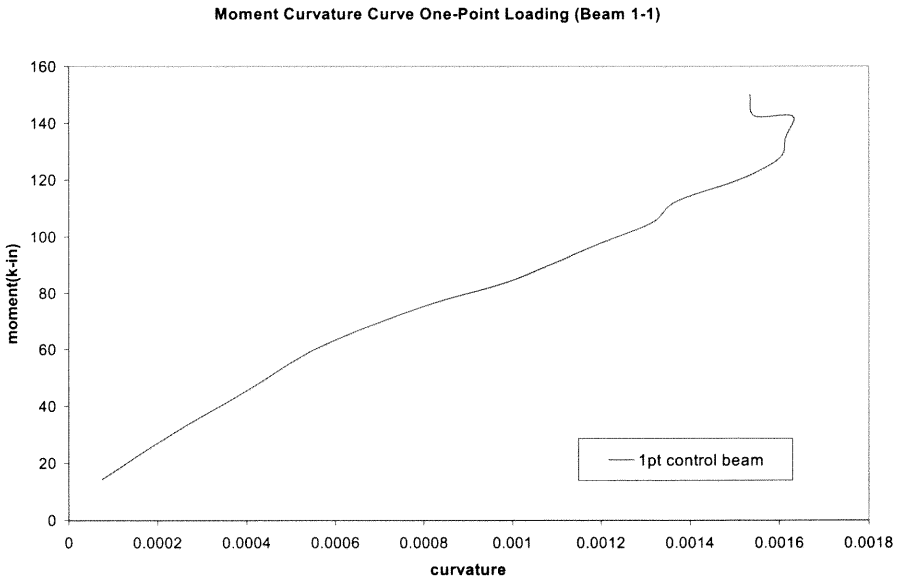

Figure D.1 Moment-curvature curve beam 1-1

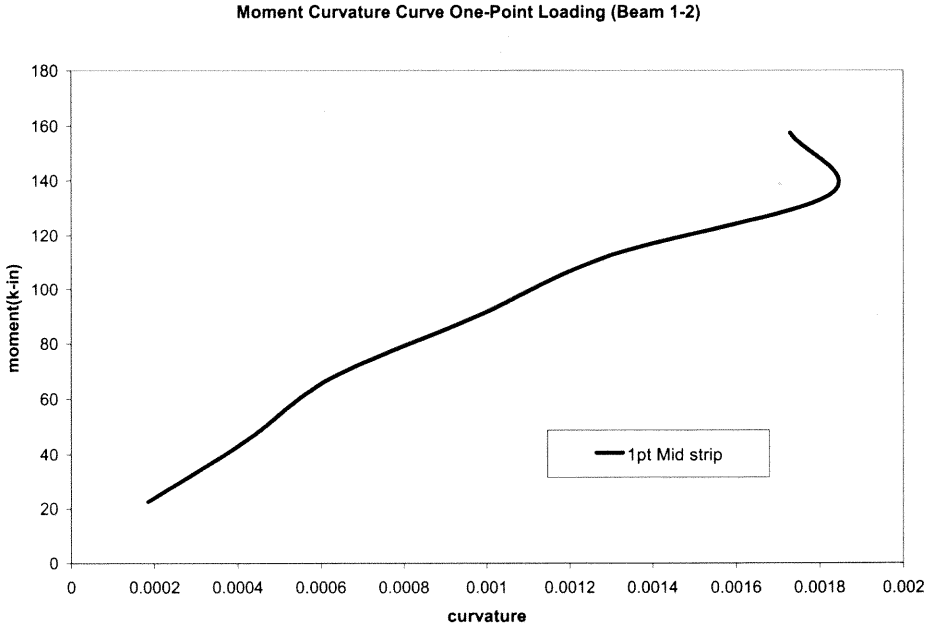

Figure D.2 Moment-curvature curve beam 1-2

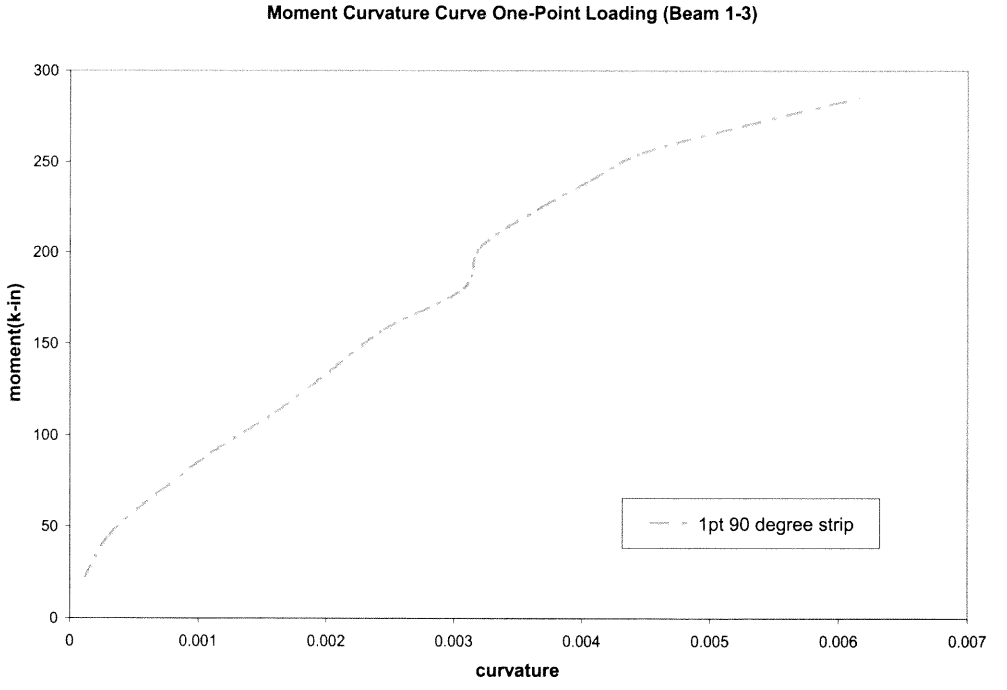

Figure D.3 Moment-curvature curve beam 1-3

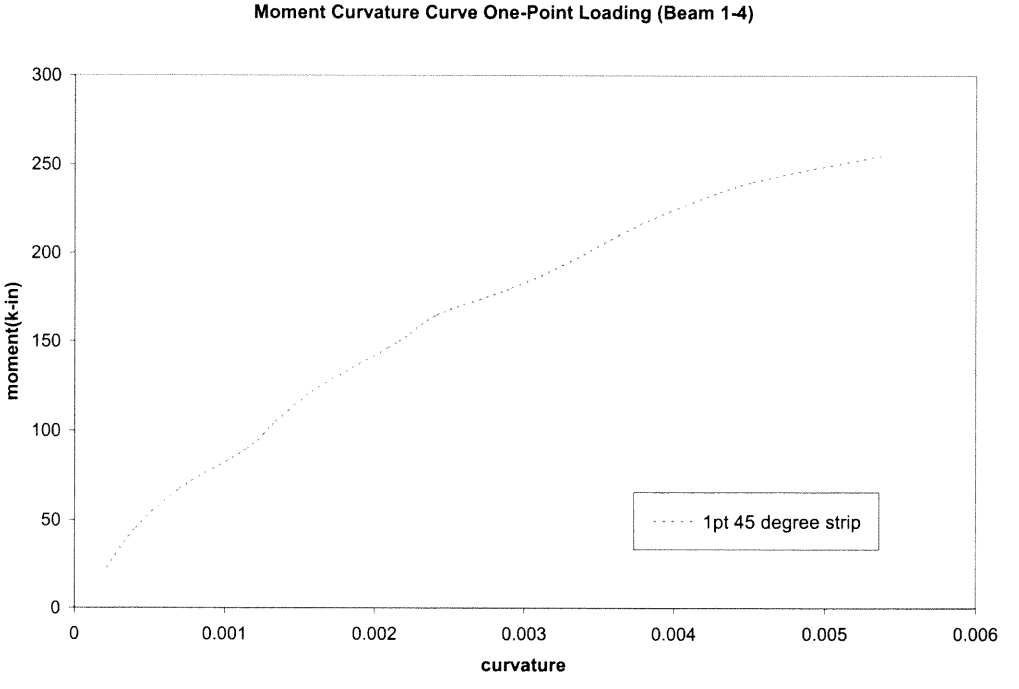

Figure D.4 Moment-curvature curve beam 1-4

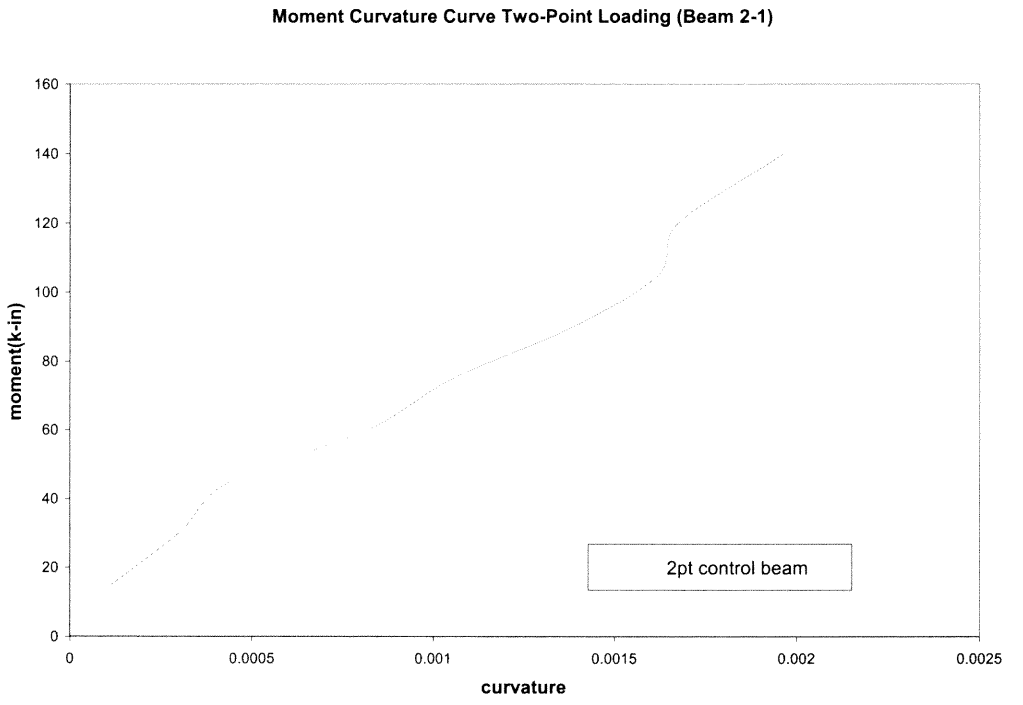

Figure D.5 Moment-curvature curve beam 2-1

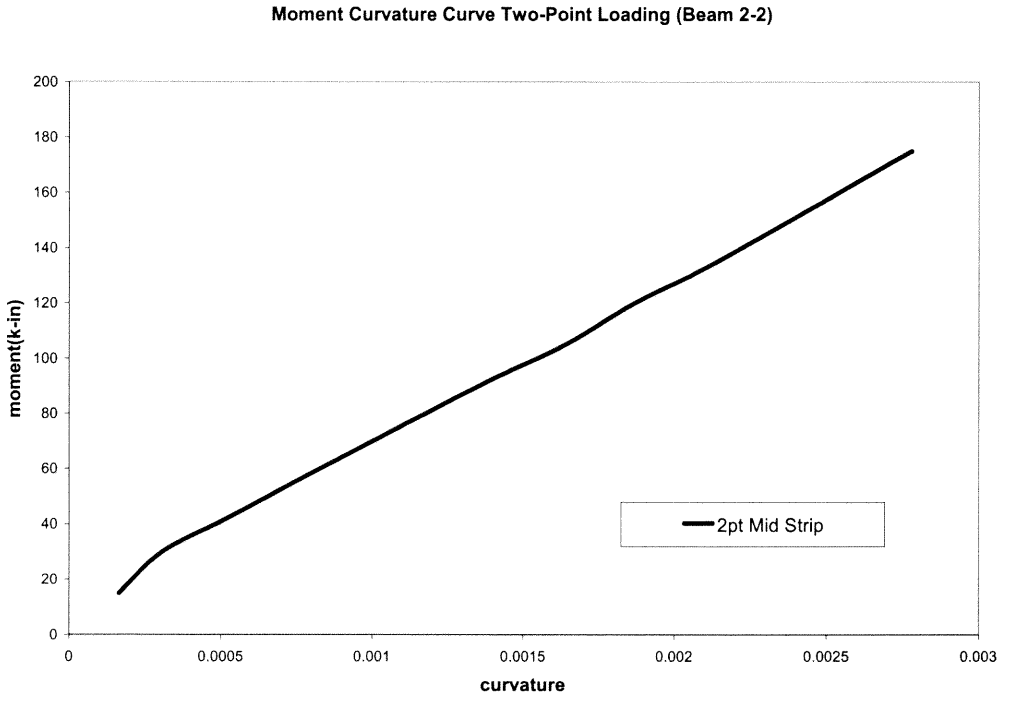

Figure D.6 Moment-curvature curve beam 2-2

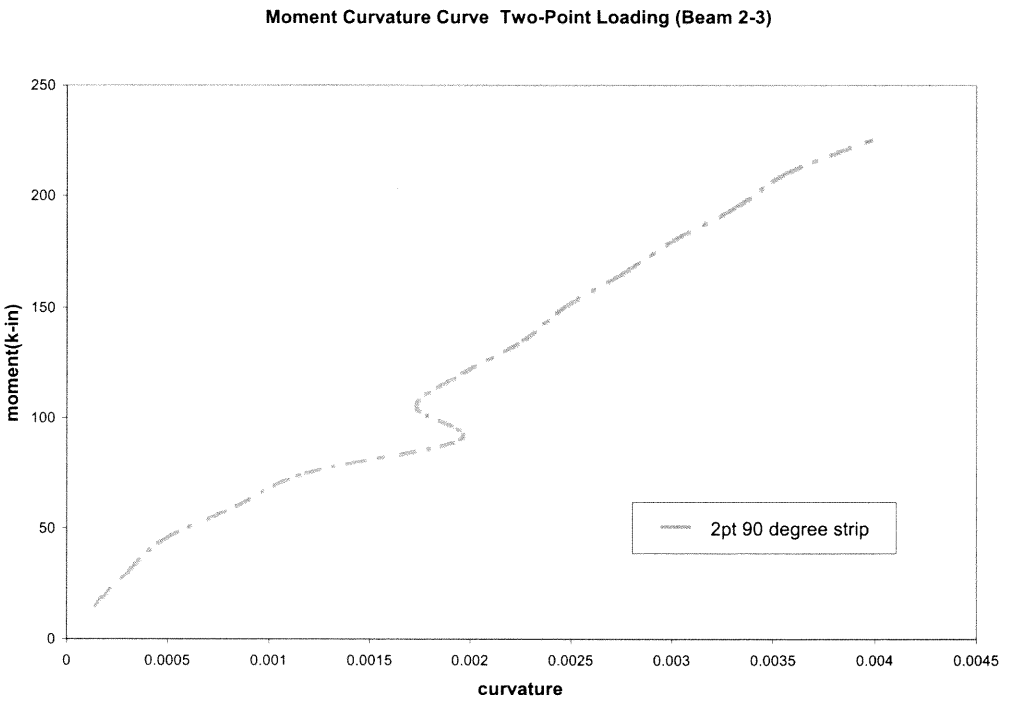

Figure D.7 Moment-curvature curve beam 2-3

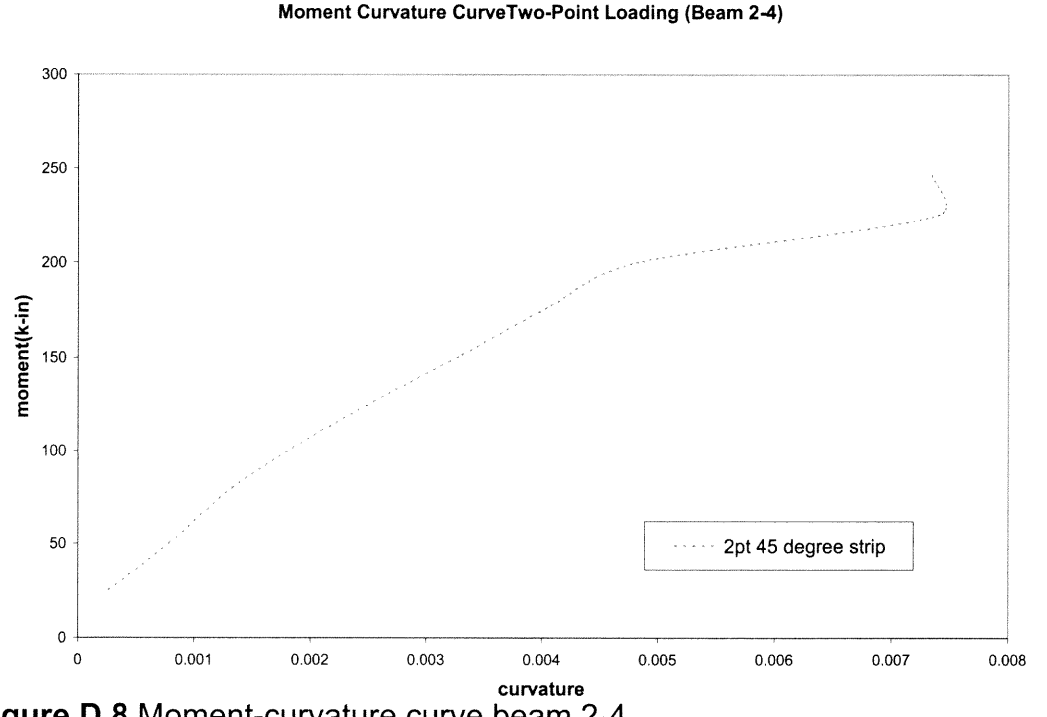

Figure D.8 Moment-curvature curve beam 2-4

REFERENCES

1. Sika Corporation Marketing Department "Sika CarboDur Composite Strengthening Systems, Engineering Guidelines for Design and Application" 201 Polito Avenue Lyndhurst, NJ. Date 8/10/99

2. Chajes, M., and Finch Jr., W., "Rehabilitation of Foulk Road bridge #26 (Wilmington, Delaware) using advanced composite materials," Research project University of Delaware.

3. Khalifa, A. and Nanni, A., "Improving shear capacity of existing RC T-sections using CFRP composites," Cement & Concrete Composites, 22, 2000, pp. 165-174

4. Taljsten, B. and Elfgren, L., "Strengthening concrete beams for shear using CFRP materials: evaluation of different application methods," Composites: part B 31, 2000, pp. 87-96

5. Zhang, Z., and Hsu, T., "Shear behavior of reinforced concrete beams strengthened by Sika CFRP laminates" Technical Report Structural series No. 2000-1

6. ACI Committee 318, "Building code requirements for structural concrete," ACI Building Code. ACI 318-99

7. Wang, C., and Salmon C. G., "Reinforced Concrete Design," 5th Edition, New York, Harper and Row, 1992

8. Sika. 1995. "Sika CarboDur High-duty CFRP Strengthening System." Product Data Sheet N.p.: n.p.

9. Sika. 1995. "Sikadur-30 Adhesive for Bonding Reinforcement." Product Data Sheet N.p.: n.p.

10. Bresler, B., and MacGregor, J. G., "Review of Concrete Beams Failing in Shear," Journal of the Structural Division, ASCE, Vol. 93, No. St-1, Feb. 1967, pp. 343-372

11. Triantafillou, T., and Antonopoulos, C., "Design of concrete flexural members strengthened in shear with FRP," Journal of Composites for Construction, ASCE Vol. 4, No 4, November, 2000, pp. 198-205

12. Binzindavyi L., and Neale K., " Transfer lengths and bond strengths for composites bonded to concrete," Journal of Composites for Construction, ASCE Vol. 3, No 4, November, 1999, pp. 153-160